REVIEW ARTICLE

Thermal equilibria and thermodynamics of trapped plasmas with a single sign of charge*

T. M. O'Neil and Daniel H. E. Dubin
University of California at San Diego, La Jolla, California 92093-0319

(Received 11 November 1997; accepted 17 February 1998)

Plasmas consisting exclusively of particles with a single sign of charge (e.g., pure electron plasmas and pure ion plasmas) can be confined by static electric and magnetic fields (e.g., in a Penning trap) and also be in a state of global thermal equilibrium. This important property distinguishes these totally un-neutralized plasmas from neutral and quasineutral plasmas. This paper reviews the conditions for and structure of the thermal equilibrium states and then develops a thermodynamic theory of the trapped plasmas. Thermodynamics provides hundreds of general relations (Maxwell relations) between partial derivatives of thermodynamic variables with respect to one another. Thermodynamic inequalities place general and useful bounds on various quantities. General and relatively simple expressions are provided for fluctuations of the thermodynamic variables. In practice, trapped plasmas are often made to evolve through a sequence of thermal equilibrium states through the slow addition (or subtraction) of energy and angular momentum (say, by laser cooling and torque beams). A thermodynamic approach to this late time transport describes the evolution through coupled ordinary differential equations for the thermodynamic variables, which is a huge reduction in complexity compared to the partial differential equations typically required to describe plasma transport. These evolution equations provide a theoretical basis for the dynamical control of the plasmas. [S1070-664X(98)00106-2]

I. INTRODUCTION

Plasmas with a single sign of charge (e.g., pure electron plasmas and pure ion plasmas) are routinely confined in Penning traps for long times (hours and even days) in states of global thermal equilibrium.[1–4] Moreover, the plasmas are made to evolve through a sequence of thermal equilibrium states by the slow addition (or subtraction) of energy and angular momentum. These experiments suggest the need for a thermodynamic theory of trapped plasmas.

The main advantage of a thermodynamic description is that it provides a huge reduction in the level of complexity required to specify the system state. Much of many body physics can be viewed as the development of such reductions (e.g., Liouville distribution→Boltzmann distribution→fluid description), and thermodynamics is the ultimate reduction. The system state is completely specified by the values of a few thermodynamic variables. However, no information is lost so long as the system is in thermal equilibrium. A complete set of thermodynamic variables fixes all of the parameters (e.g., temperature) in the Gibbs distribution.

We will see the power of this reduction in Sec. VI where we discuss a thermodynamic approach to transport. This theory applies when the evolution is slow enough that the plasma passes through a sequence of thermal equilibrium states. The plasma evolution is then governed by coupled ordinary differential equations for the time dependence of the thermodynamic variables, which is a huge reduction in complexity relative to the partial differential equations typically required to describe plasma transport.

Although thermodynamics plays an important role in much of many body physics (e.g., in condensed matter physics), it has not been used to describe neutral (or quasineutral) trapped plasmas. The reason for this apparent omission is easy to understand. Such plasmas cannot be confined by static electric and magnetic fields and also be in a state of global thermal equilibrium,[5] so a thermodynamic description is simply not available. The possibility of a thermodynamic description is an important property that distinguishes plasmas with a single sign of charge from their neutral (and quasineutral) cousins.

There is some previous work[6–10] on the thermodynamics of trapped plasmas with a single sign of charge, but it is limited in focus and scope and is not intended to be a general development of the subject. For example, it focuses on the special case of long plasma columns (formally, infinitely long or shaped like a right circular cylinder) and does not develop and exploit Maxwell relations, thermodynamic inequalities, etc. Here, we provide a general development of the subject that allows for realistic plasma configurations, uses the natural thermodynamic variables for the trapped plasma systems, and develops and applies the full thermodynamic formalism.

*This review paper is based in part on the Maxwell Prize lecture given by Professor O'Neil at the 1996 annual meeting of the Division of Plasma Physics in Denver, Colorado.

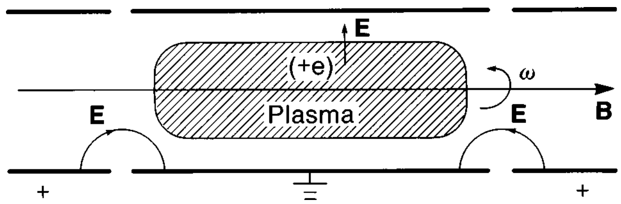

FIG. 1. Schematic diagram of a Malmberg–Penning trap.

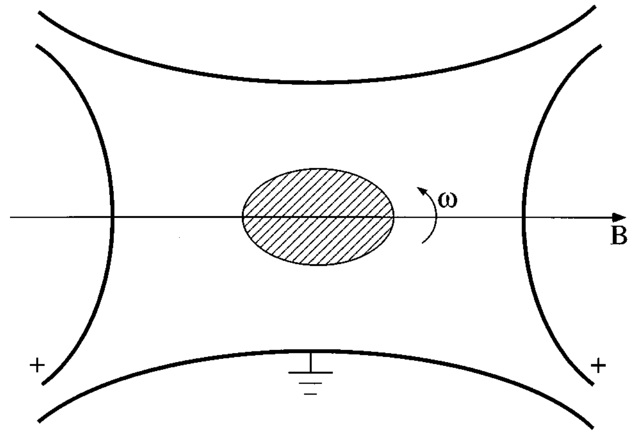

FIG. 2. Penning trap for which the electrodes are hyperbolas of revolution.

Sections II and III review the confinement geometry, constants of the motion, and the conditions for and structure of the thermal equilibrium states for the trapped plasmas. Section IV develops the general theory of thermodynamics for these systems. Section V considers the special case of large trapped plasmas, and shows that the thermodynamic functions for these systems are simply related to those for an infinite homogeneous one component plasma (OCP), which are well known even in the limit of strong correlation.[11,12] Section VI develops the thermodynamic approach to transport and applies it to explain observations in recent experiments.[2] Section VII notes that in some special configurations the center-of-mass motion decouples from the other degrees of freedom. This introduces new constants of the motion, which then enter as new thermodynamic variables. The thermodynamic theory of transport then describes a dynamical evolution in which the center-of-mass motion is coupled to the other thermodynamic variables. This generalized theory is used to describe a limit cycle behavior observed in the late time dynamics of trapped pure electron plasmas.[13]

II. CONFINEMENT AND CONSTANTS OF THE MOTION

Figure 1 shows a simple example of a Penning trap.[14] A conducting cylinder is divided axially into three sections with the central section held at ground potential and the two end sections held at positive potential. (Throughout the paper, the figures and discussion refer to positively charged particles, but the case of negative charges is covered by obvious sign changes.) Also, there is a uniform axial magnetic field. The plasma resides in the region of the central grounded section with radial confinement provided by the magnetic field and axial confinement by the electric fields. To understand radial force balance, one must realize that the plasma rotates about the axis of symmetry of the trap. The associated Lorentz force $(e\mathbf{v}\times\mathbf{B}/c)$, where $\mathbf{v}$ is the rotational velocity, is directed radially inward and balances all of the radially outward forces (centrifugal, pressure, and electrostatic). This simple form of the trap (with cylindrical electrodes) is often called a Malmberg–Penning trap.[15] Figure 2 shows a Penning trap in which the cylindrical electrodes are replaced by hyperbolas of revolution.[16,17] Such traps were developed originally to confine small numbers of charged particles, but more recently have been used to confine charge clouds that are large and dense enough to qualify as a plasma. We will develop the theory so that it is broad enough to encompass both of these traps.

As a preliminary to a discussion of the thermal equilibrium states, it is necessary to determine the effective constants of the motion for the plasma. These quantities need not be exact constants; it is only necessary that they be nearly constant on the time scale required for interactions to bring the plasma charges into thermal equilibrium with each other. For our theoretical discussion, we introduce an idealized model of the plasma and trap such that the quantities of interest are exact constants.

We consider a plasma of N like charges that interact electrostatically in a cylindrically symmetric Penning trap with time-independent voltages applied to the electrodes and a time-independent and uniform axial magnetic field, $\mathbf{B}=\hat{z}B$. There may be more than three electrodes, and all of the electrodes together completely bound the confinement region so that the interior solution to Poisson's equation is well defined. The vector potential for the uniform magnetic field can be written as $\mathbf{A}=\hat{\theta}A_\theta(r)$, where $A_\theta(r)=Br/2$. Here (r,θ,z) is a cylindrical coordinate system with the z axis coincident with the axis of symmetry of the trap. We write the electric potential as

$$\phi(\mathbf{r})=\phi_T(\mathbf{r})+\sum_j eG(\mathbf{r}|\mathbf{r}_j), \tag{1}$$

where $\phi_T(\mathbf{r})$ is the trap potential in the absence of a plasma. This potential satisfies Laplace's equation and matches the potential specified on the conducting boundary, that is, on the electrodes. The quantity $G(\mathbf{r}|\mathbf{r}_j)$ is the Green's function that vanishes on the conducting boundary, and $\mathbf{r}_j$ is the position of the jth charge. The Green's function differs from the Coulomb interaction $1/|\mathbf{r}-\mathbf{r}_j|$ because of image charges in the conducting boundary.

To a good approximation, the motion of the charges is governed by the Hamiltonian

$$H=\sum_{j=1}^{N}\left(\frac{p_{r_j}^2}{2m}+\frac{[p_{\theta_j}-(e/c)A_\theta(r_j)r_j]^2}{2mr_j^2}+\frac{p_{z_j}^2}{2m}\right)+\sum_{j=1}^{N}e\phi_T(\mathbf{r}_j)+\frac{1}{2}\sum_{i,j=1}^{N}{}' e^2G(\mathbf{r}_i|\mathbf{r}_j), \tag{2}$$

where the canonical momenta are given by

$$p_{r_j}=m\dot{r}_j\,,\quad p_{\theta_j}=mr_j^2\dot{\theta}_j+\frac{e}{c}A_\theta(r_j)r_j\,,\quad p_z=m\dot{z}_j\,. \tag{3}$$

The first sum is the kinetic energy, the second is the electrostatic energy of the charges in the trap potential, and the third is the electrostatic interaction energy of the charges with each other and with their images. Diamagnetic and relativistic effects have been neglected since velocities are typically small (i.e., $|\mathbf{v}_j|/c\ll 1$) in the experiments of interest. Also, in the second sum, we have neglected the interaction energy of each charge with its own image; typically this is much smaller than $e\phi_T(\mathbf{r})$ unless the charge is very near the wall. Note that the interaction of a particular charge with the images of all of the other charges can be large and is retained in the third sum. The constants of the motion follow from the symmetry properties of the Hamiltonian, and these properties are not changed by dropping the $(v/c)^2$ corrections and the interaction of a charge with its own image. These approximations are used only to simplify the notation. Also, for notational simplicity, we have taken the case of a single species plasma; the results are easily generalized to a multispecies plasma so long as all of the species have the same sign of charge.

Since the Hamiltonian is invariant under translations in time (i.e., $\partial H/\partial t=0$), the Hamiltonian itself is a constant of the motion

$$H=E. \tag{4}$$

We may think of H as the total particle energy, but should note that H is not the same as the "system energy," i.e., the energy required to assemble the plasma in the trap. If for simplicity we fix the voltages on the electrodes and the current in the solenoid, and do not include in our considerations the energy required to charge the electrodes and the solenoid in the absence of the plasma, the system energy equals H plus the work done by external circuits as the plasma is assembled. For example, as charges are brought from infinity into the trap, image charges flow onto the electrodes, doing work against the circuits holding the electrode voltages fixed. Also, work is required of the circuits holding the solenoid current fixed due to the mutual inductance between the plasma and the solenoid. This will be discussed in detail in Sec. IV B, where it is the basis for our discussion of thermodynamic stability of non-neutral plasmas.

The cylindrical symmetry of the apparatus implies that the trap potential is of the form $\phi_T(\mathbf{r}_j)=\phi_T(r_j,z_j)$ and that the Green's function is of the form $G(\mathbf{r}_i|\mathbf{r}_j)=G(r_i,z_i,r_j,z_j,\theta_i-\theta_j)$. Thus the Hamiltonian is invariant under translations in θ (i.e., $\Sigma_{j=1}^N\partial H/\partial\theta_j=0$), and the total canonical angular momentum is conserved

$$P_\theta=\sum_{j=1}^N p_{\theta_j}=L. \tag{5}$$

Of course, for a real plasma in a real trap, the total energy and the total canonical angular momentum are not conserved exactly. The charges slowly radiate away both energy and angular momentum; there are neutrals, and collisions with the neutrals change the plasma energy and angular momentum; and most importantly there are small field errors and construction errors that break the cylindrical symmetry and apply a small torque on the plasma. However, with care all of these effects can be made sufficiently small that interactions between the particles bring the plasma into thermal equilibrium before the energy and angular momentum change by a significant amount. Thus we proceed with a description of the plasma confinement and thermal equilibrium states using our idealized model.

To understand the confinement, it is useful to introduce the Hamiltonian in a frame that rotates with frequency $-\omega$; this quantity is given by[18]

$$H_R=H+\omega P_\theta, \tag{6}$$

and is conserved so long as H and P_θ are conserved. Of course, we are free to view the dynamics from any rotating frame that is convenient. It is important to note here that $-\omega$ is not necessarily the rotation frequency of the plasma. The minus sign is included explicitly so that ω can be chosen to be positive (for a plasma of positive charges). When the canonical momenta are replaced with velocity variables, Eq. (6) takes the form

$$H_R=\sum_{j=1}^N\frac{m}{2}v_j^2+\sum_{j=1}^N e\phi_T(r_j,z_j)+\frac{1}{2}\sum_{i,j=1}^{N}{}' e^2G(\mathbf{r}_i|\mathbf{r}_j)$$
$$+\omega\sum_{j=1}^N\left(mv_{\theta_j}r_j+\frac{e}{c}Br_j^2/2\right), \tag{7}$$

where we have used $(e/c)A_\theta(r)r=eBr^2/2c$. Carrying out a small amount of algebra yields the result

$$H_R=\sum_{j=1}^N\frac{m}{2}(\mathbf{v}_j+\omega r_j\hat{\theta}_j)^2+\sum_{j=1}^N e\phi_R(r_j,z_j)$$
$$+\frac{1}{2}\sum_{i,j=1}^{N}{}' e^2G(\mathbf{r}_i|\mathbf{r}_j), \tag{8}$$

where

$$e\phi_R(r,z)=e\phi_T(r,z)+m\omega(\Omega_c-\omega)r^2/2 \tag{9}$$

is the effective trap potential in the rotating frame and $\Omega_c=eB/mc$ is the cyclotron frequency.

This potential consists of three terms: $e\phi_T$ is the potential energy due to the voltages maintained on the electrodes, $-m\omega^2r^2/2$ is the centrifugal potential, and $m\omega\Omega_cr^2/2=\int_0^r dr\; e(\omega r)B/c$ is the potential that is induced by rotation through the magnetic field. It is this last term that provides the radial confinement. For a suitable choice of the bias voltage on the end electrodes and for sufficiently large $\omega(\Omega_c-\omega)$, the equipotential surfaces of $e\phi_R(r,z)$ are nested surfaces of revolution with the value of $e\phi_R(r,z)$ increasing outward from the center of the trap. The term $e\phi_T(r,z)$ increases as z moves toward either end where the positively biased end electrodes are located. For sufficiently large $\omega(\Omega_c-\omega)$, the term $m\omega(\Omega_c-\omega)r^2/2$ makes $e\phi_R(r,z)$ an increasing function of r [even though $e\phi_T(r,z)$ is decreasing in r]. Thus $e\phi_R(r,z)$ is a potential well that acts to confine the plasma.

A simple confinement theorem can be constructed by noting that the first and third sums in Eq. (8) are non-negative. The non-negative character of the third sum follows from the fact that $G(\mathbf{r}|\mathbf{r}')>0$. A negative value for $G(\mathbf{r}|\mathbf{r}')$ would imply that $G(\mathbf{r}|\mathbf{r}')$ reaches a minimum at some point $\mathbf{r}$ inside the confinement region; recall that $G(\mathbf{r}|\mathbf{r}')$ vanishes on the boundary and is positive near $\mathbf{r}=\mathbf{r}'$. Of course, a minimum is not possible since $\nabla^2 G(\mathbf{r},\mathbf{r}')=0$ except at $\mathbf{r}=\mathbf{r}'$.

Particles can escape to the wall only by climbing high up in the potential well, that is, by increasing the second sum in Eq. (8). This must be accompanied by a decrease in the other two sums, since H_R is conserved. Physically, the particles can climb up the potential only by using kinetic energy and electrostatic energy of interaction. Because these latter two quantities are non-negative, their initial values set the maximum amount that they can decrease. Suppose that all of the particles are initially inside (bounded by) some equipotential surface $e\phi_R(r,z)=e\phi_1$ and that the first equipotential where the potential begins to decrease (or intersects the wall) is $e\phi_R(r,t)=e\phi_2$. Then only a small fraction of the charges can escape if $Ne(\phi_2-\phi_1)$ is much larger than the initial values of the first and third sums in Eq. (8).

In applying this theorem, we are free to choose ω. However, care must be taken, since ω appears both in the effective trap potential and in the kinetic energy (in the rotating frame). Also, ω must lie in the interval $0<\omega<\Omega_c$ so that $\omega(\Omega_c-\omega)$ is positive. Nevertheless, for any initial state of the plasma, the well can be made deep enough to provide confinement for a range of ω values, if Ω_c and the bias voltage on the end electrodes are sufficiently large.

III. THERMAL EQUILIBRIUM STATES

A. Distribution function

Given that the particles remain confined, Coulomb interactions between the particles must bring the plasma to a state of thermal equilibrium. For a thermal equilibrium plasma characterized by the fixed values $H(\mathbf{r}_1,\mathbf{v}_1,\ldots,\mathbf{r}_N,\mathbf{v}_N)=E$ and $P_\theta(\mathbf{r}_1,\mathbf{v}_1,\ldots,\mathbf{r}_N,\mathbf{v}_N)=L$, the $6N$-dimensional particle distribution is the distribution for a microcanonical ensemble[19]

$$f_{mc}(\mathbf{r}_1,\mathbf{v}_1,\ldots,\mathbf{r}_N,\mathbf{v}_N)=A\,\delta[H-E]\,\delta[P_\theta-L], \qquad (10)$$

where A is a constant that is chosen to normalize the phase-space integral of the distribution to unity. According to the ergodic hypothesis, the average of any function $G(\mathbf{r}_1,\mathbf{v}_1,\ldots,\mathbf{r}_N,\mathbf{v}_N)$ taken over the microcanonical distribution is equal to the long time average of the function taken along the system trajectory in the $6N$-dimensional phase space.

We will consider plasmas with enough particles ($N\gg1$) that the distribution for a microcanonical ensemble is well approximated by the distribution for a canonical ensemble (the Gibbs distribution)[19,20]

$$f_c(\mathbf{r}_1,\mathbf{v}_1\ldots,\mathbf{r}_N,\mathbf{v}_N)=C\,\exp[-(H+\omega P_\theta)/kT], \qquad (11)$$

where C is a factor used to normalize the integral of f_c to unity. Formally the Gibbs distribution describes a plasma

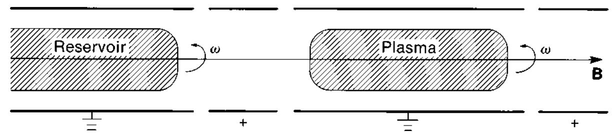

FIG. 3. Plasma in thermal contact with heat and angular momentum reservoir.

that is in thermal contact with an energy and angular momentum reservoir. For example, Fig. 3 shows a trapped plasma that is in thermal contact with an infinitely long column (the reservoir). It is characterized by temperature T and rotation frequency $-\omega$. Thermal fluctuations produce a transfer of energy and angular momentum back and forth between the reservoir and plasma. However, for a sufficiently large plasma (i.e., $N\gg1$), the fluctuations in plasma energy and angular momentum are small compared to the mean energy and angular momentum and have only a small influence on the plasma state. Thus for most physical quantities, an average over the microcanonical distribution can be replaced by an average over the Gibbs distribution.[20] In establishing the correspondence between the two distributions, T and ω are chosen so that $E=\langle H\rangle$ and $L=\langle P_\theta\rangle$, where the averages are over the Gibbs distribution. This well-known equivalence between the two distributions is useful because the Gibbs distribution offers advantages analytically; for example, H and P_θ enter the Gibbs distribution only through the combination $H_R=H+\omega P_\theta$. However, we should note that the equivalence does not extend to averages of certain fluctuations; for example, $\langle(H-E)^2\rangle$ is identically zero for the microcanonical distribution and is small [i.e., $\langle(H-E)^2/E^2\rangle\sim1/N$] but nonzero for the Gibbs distribution.

From Eq. (8), one can see that the velocity dependence of f_c is a product of Maxwellians in a frame that rotates with frequency $-\omega$. Thus the local fluid velocity $\langle\mathbf{v}\rangle=\omega r\hat{\theta}$ is a shear-free rigid rotor flow. Of course, a thermal equilibrium flow must be shear-free; viscous forces acting on a shear in the flow would produce entropy, and that is impossible for a state of maximum entropy. One should note the distinction between the meanings of ω here and in the confinement theorem. Here ω is the rotation frequency of the plasma as determined by the values of $E=\langle H\rangle$ and $L=\langle P_\theta\rangle$; whereas, in the confinement theorem, ω is the rotation frequency of some arbitrary frame from which we choose to view the dynamics.

To see that distribution (11) describes a confined plasma, we note that the probability of finding a particle high up in the potential well, that is, where $e\phi_R(r,z)$ is large, is exponentially small. The electrode surfaces are assumed to be well outside the surface where the density becomes exponentially small. The existence of thermal equilibrium states for confined plasmas with a single sign of charge has been known for many years.[21–24]

Note that the confinement works only for a plasma with a single sign of charge. In the effective trap potential [see Eq. (9)], the two terms that provide confinement [i.e., $e\phi_T$ and $m\omega\Omega_c r^2/2$] both enter with the sign of the change as a coefficient; so confinement of positive charges implies nonconfinement of negative charges. As mentioned earlier, it is well known that a neutral or quasineutral plasma cannot be confined by static electric and magnetic fields and also be in a state of global thermal equilibrium. Such a plasma cannot be confined and also be in a state of minimum free energy; there is always free energy to drive instabilities. In contrast, distribution (11) describes a totally un-neutralized plasma that is confined stably forever, at least for our ideal model where E and L are exact constants of the motion.

This is a good point to return to the fact that E and L are not exactly constant for a real plasma in a real trap. As mentioned earlier, various effects (radiation, collisions with neutrals, and interactions with field errors and construction errors that break the cylindrical symmetry) produce slow changes in E and L. However, by using a high-quality vacuum and by constructing the trap with a high degree of cylindrical symmetry, E and L can be nearly constant on the time scale required for Coulomb collisions to bring the charges into thermal equilibrium with each other. Thus distribution (11) still provides a correct description of the plasma state, but the slow evolution of E and L translates to a slow evolution of T and ω. If no counter measures were taken, the ambient heating and ambient torque (typically a drag that opposes the plasma rotation) would cause T and ω to change in such a way that the plasma would be lost to the wall. However, counter measures such as laser cooling and laser torques can be used to maintain E and L (and therefore T and ω) at constant values indefinitely. Alternatively, E and L can be deliberately varied so that the plasma sweeps through a sequence of thermal equilibrium states.[1,2] Such an evolution will be discussed in Sec. III C.

B. Relation to a one-component plasma

The Gibbs distribution for the trapped plasma is equivalent to that for a one-component plasma (OCP).[24] An OCP is a system of point charges embedded in a uniform neutralizing background charge.[11,12] The infinite homogeneous OCP has been a favorite theoretical model for the study of correlation effects, and its thermodynamic properties are well known. In Sec. V, we will relate the thermodynamic functions of an infinite homogeneous OCP to those of a large trapped plasma. Here we use the equivalence between the systems to help understand the spatial structure of the trapped plasmas.

To demonstrate the equivalence, we first note from Eq. (9) that the second term in $e\phi_R(r,z)$ is quadratic in r. As described earlier, this term provides the correction due to rotation. Suppose that the radial confinement were not provided by rotation through a magnetic field but rather by an imaginary cylinder of uniform negative charge (to confine a plasma of positive charges). Such a charge distribution would produce a radial electric field $E_r=-2\pi e n_- r$ and an electric potential $\phi_-=\pi e n_- r^2$, where $n_-=$constant is the density of the imaginary negative charge. If this charge density were chosen to have the value $en_-=m\omega(\Omega_c-\omega)/2\pi e$, the cylinder of negative charge would provide a potential-energy term $e\phi_-=m\omega(\Omega_c-\omega)r^2/2$ that is identical to the second term in $e\phi_R$. Thus the Gibbs distribution for the two systems would differ only by rotation, that is, by the velocity shift $\mathbf{v}_j\rightarrow\mathbf{v}_j+\omega r_j\hat{\theta}_j$. The spatial dependence, including all correlations, would be identical.[24]

We know what would happen if we put a collection of positive charges into a potential well produced by the cylinder of uniform negative charge (and the electrode potentials). The positive charges would go to the bottom of the well and match their density to that of the negative charge (i.e., $n=n_-$), neutralizing the negative charge out to some surface of revolution where the supply of positive charges was exhausted. The condition $n=n_-$ is typically written as[23]

$$\omega_p^2=2\omega(\Omega_c-\omega), \tag{12}$$

where $\omega_p^2=4\pi n e^2/m$ is the square of the plasma frequency.

An alternate form of this argument starts from the observation that the plasma charges must arrange themselves so that any external electric field is Debye shielded out when viewed in the plasma rest frame (here, the rotating frame of the plasma). The effective external field in this frame is $-\nabla\phi_R$, so we conclude that

$$\phi_R(\mathbf{r})+\phi_p(\mathbf{r})=\text{const} \tag{13}$$

in the plasma interior, where $\phi_p(\mathbf{r})$ is the plasma space-charge potential.[1,25] Equation (12) then follows from Poisson's equation, $\nabla^2\phi_p=-4\pi e n$, plus the relation $\nabla^2\phi_R=4\pi e n_-$. Here we have used the fact that ϕ_T is a vacuum field.

In these arguments we have introduced the density $n(\mathbf{r})$ and the space-charge potential $\phi_p(\mathbf{r})$. Formally, these quantities are related to Gibbs distribution (11) through the integrals

$$n(\mathbf{r}_1)=\int d^3\mathbf{v}_1\cdots d^3\mathbf{r}_N d^3\mathbf{v}_N f_c \tag{14}$$

and

$$\phi_p(\mathbf{r})=\int d^3\mathbf{r}'\, G(\mathbf{r}|\mathbf{r}')n(\mathbf{r}'), \tag{15}$$

where $G(\mathbf{r}|\mathbf{r}')$ is the Green's function introduced in Eq. (1).

This general picture of a plasma that is uniform density out to a surface of revolution where the density drops to zero in a thin surface sheath has been verified by detailed numerical solutions[23,26] and by experiment.[1,3,27] The influence of the surface extends into the plasma about a correlation length, so the surface sheath is about a correlation length thick. For a weakly correlated plasma, the correlation length is of order the Debye length, $\lambda_D=(kT/4\pi n e^2)^{1/2}$, and the density drops monotonically to zero on this scale length. For a strongly correlated plasma, the density does not fall monotonically to zero, but suffers oscillations near the surface. The density is concentrated on nested shells. One can think of these shells as crystal planes that are deformed to follow the contour of the surface. The shell structure extends into the plasma a correlation length; which is a few times the interparticle spacing $n^{-1/3}$ for a plasma in the fluid state, but can be substantially larger for a plasma in a crystal state. Because of the curvature of the surface, one expects dislocations near the surface and a ''surface correlation length'' that is reduced significantly from the bulk correlation length for an infinite homogeneous crystal. Numerical simulations[26] suggest a ''surface correlation length'' that is a few tens of interparticle spacings. We will refer to a plasma as large when the thickness of the surface sheath is much smaller than all three plasma dimensions. In this case, the volume of the surface sheath is small compared to the total plasma volume, and we can relate the thermodynamic functions of the trapped plasma to those of an infinite homogeneous OCP (see Sec. V). For a weakly correlated plasma or a plasma in the fluid state the criterion that the plasma be large is easily satisfied, but for a crystal state where the shell structure extends into the plasma for tens of interparticle spacing the criterion is quite demanding.

For some experiments with pure electron plasmas, the temperature is low enough and the magnetic field large enough that the cyclotron motion is quantized (i.e., $\hbar\Omega_c \sim kT$). Although the argument concerning the equivalence between the Gibbs distributions for a trapped plasma and for an OCP is classical, one can construct an equivalent quantum mechanical argument provided that thermal deBroglie wavelength $\sqrt{\hbar^2/mkT}$ is small compared to the interparticle spacing.[28]

C. Spheroidal plasmas

There is an important special case where the shape of the surface of revolution can be determined analytically. The plasma is small compared to the dimensions of the trap and resides in a nearly quadratic trap potential. As we will see, the surface of revolution is then a spheroid (an ellipse of revolution).[1,25]

Near the center of a trap, one expects (by Taylor expansion) that the trap potential is approximately quadratic

$$e\phi_T \simeq \frac{m\omega_z^2}{2}(z^2 - r^2/2) + C, \tag{16}$$

where ω_z^2 and C are constants. The coefficient of r^2 relative to that of z^2 is determined by the requirement $\nabla^2\phi_T = 0$. Some traps are designed to make the quadratic approximation much better than would in general be expected. For example, Fig. 2 shows a trap for which the conducting electrodes are hyperbolas of revolution. Since the equipotential surfaces for the quadratic potential [i.e., $z^2 - r^2/2 = \text{const}$] define hyperbolas of revolution, a trap for which the hyperbolas extended to infinity would produce an exactly quadratic potential. In practice, the hyperbolas are truncated, as shown in Fig. 2, so the quadratic form is only an approximation, though it is very good over a substantial region near the center of the trap. If the equation defining the cap electrodes is $z^2 - r^2/2 = z_0^2$, the equation defining the center ring electrode is $z^2 - r^2/2 = -r_0^2/2$, and the potential difference between cap and ring electrodes is V_0, the frequency ω_z is given by

$$eV_0 = \frac{m\omega_z^2}{2}(z_0^2 + r_0^2/2). \tag{17}$$

Even for a trap with cylindrical electrodes, it is possible to achieve a potential that is nearly quadratic over a substantial region.[17] This is accomplished by choosing the lengths of the various cylinders so that the quartic term in the Taylor series vanishes; the cubic and quintic terms vanish by symmetry.

Adding $m\omega(\Omega_c - \omega)r^2/2$ to ϕ_T yields the effective trap potential in the rotating frame

$$e\phi_R(r,z) = \frac{m\omega_z^2}{2}(z^2 + \beta r^2) + C, \tag{18}$$

which is also quadratic. The parameter β is defined as

$$\beta = \frac{\omega(\Omega_c - \omega)}{\omega_z^2} - \frac{1}{2} = \frac{1}{4}\frac{(\Omega_c^2 - \Omega_v^2)}{\omega_z^2} - \frac{1}{2}, \tag{19}$$

where $\Omega_v \equiv \Omega_c - 2\omega$ is the vortex frequency. The parameter β determines the symmetry of the effective trap potential, and hence the shape of the plasma. For example, when $\beta = 1$ the plasma is spherically symmetric, whereas for $\beta \gg 1$ the plasma is squeezed into a line along the z axis, and for $\beta \to 0$ the plasma is a flat two-dimensional (2D) pancake in the x-y plane.

The quadratic form of $\phi_R(r,z)$ allows one to determine the shape of the plasma.[1,2,25] As discussed earlier the plasma charges adjust their positions so that $\phi_R + \phi_p$ is constant inside the plasma. Thus the plasma space-charge potential must be quadratic within the plasma. It is well known that a uniformly charged spheroid (ellipse of revolution) in free space produces an interior potential that is quadratic in r and z and an exterior potential that approaches zero at infinity. Here the plasma dimensions are small compared to the distance to the walls, so the boundary condition that $\phi_p = 0$ on the conducting walls reduces approximately to the condition that ϕ_p approaches zero at infinity. Thus the bounding surface of the plasma is a spheroid. By writing down the potential due to a uniformly charged spheroid and comparing the coefficients of r^2 and of z^2 to the corresponding coefficients in $-\phi_R$, we obtain the relations

$$g(\alpha) = \frac{1}{2\beta + 1}, \tag{20}$$

$$\frac{\omega_p^2}{\omega_z^2} = 2\beta + 1, \tag{21}$$

where $\alpha = Z_p/R_p$ is the aspect ratio of the spheroid, $2R_p$ is the spheroid diameter, and $2Z_p$ is the length. Equation (21) is equivalent to Eq. (12), and the function $g(\alpha)$ is given by

$$g(\alpha) = Q_1^0(\alpha/\sqrt{\alpha^2 - 1})/(\alpha^2 - 1), \tag{22}$$

where Q_1^0 is an associated Legrendre function of the second kind. The aspect ratio α is a monotonically increasing function of β, as one would expect on the basis of the physical arguments following Eq. (19).

For a uniform density spheroid, the number of particles is given by

$$N = \frac{4}{3}\pi n Z_p R_p^2, \tag{23}$$

so for given N the plasma radius and half length can be written separately as

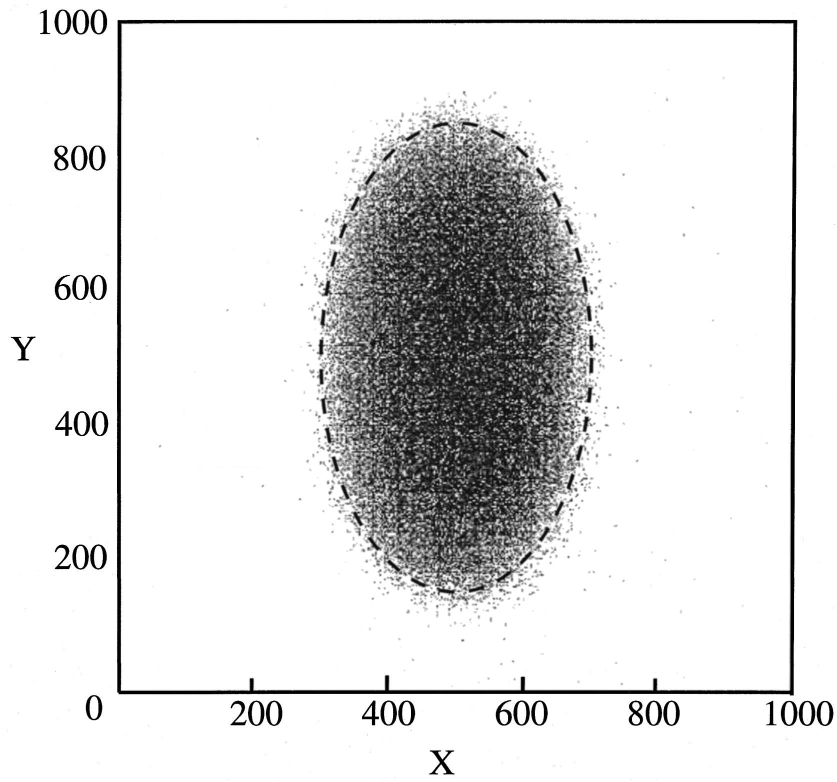

FIG. 4. Side view of Be^+ plasma, together with fitted ellipse (the dashed line). Provided by Huang, Tan, Bollinger, and Wineland of the NIST storage group (Ref. 29).

$$R_p = a_0 \left[\frac{3}{2\beta+1} \frac{N}{\alpha(\beta)} \right]^{1/3}, \tag{24}$$

$$Z_p = \alpha(\beta) R_p. \tag{25}$$

Here $a_0 \equiv (e^2/m\omega_z^2)^{1/3}$ and use has been made of Eqs. (20) and (21).

This is a good point to make contact with experiment. Figure 4 shows a side view image of a plasma of $N \simeq 8 \times 10^4$ Be^+ ions in a quadratic trap potential together with a fit to an ellipse. The picture was obtained by Huang, Tan, Bollinger, and Wineland of the National Institute of Science and Technology (NIST) ion storage group by simply imaging the fluorescence from the laser excited Be^+ ions.[29] The aspect ratio of the fitted ellipse is $\alpha = 1.763$, which agrees to better than 1% with the aspect ratio $\alpha = 1.75$ predicted from Eqs. (19) and (20) for the independently measured frequencies $\omega_z/2\pi = 754$ kHz, $\Omega_c/2\pi = 7.608$ MHz, and $\omega/2\pi = 213.7$ kHz.

In similar experiments by this group,[1,2] cooling and torque lasers (see Sec. VI) were used to control the plasma energy and angular momentum so that the plasma rotation frequency varied through the full range of allowed values, $\omega = \omega_m$ to $\omega = \Omega_c - \omega_m$. Here $\omega_m = \Omega_c/2 - [(\Omega_c/2)^2 - \omega_z^2/2]^{1/2}$ is the single-particle magnetron frequency (drift frequency), and the range of values follows from Eq. (19) plus the requirement that $\beta > 0$. The torque laser changed the angular momentum of the plasma and also did work on the plasma, since the torque was applied to a rotating plasma. As the plasma evolved, this work appeared as a change in the electrostatic energy, kinetic energy of rotation, and heat, but the cooling laser was able to remove the heat fast enough that the temperature (and Debye length) remained reasonably small.

Figure 5, taken from Bollinger *et al.*,[1,2] shows a plot R_p/R_B versus ω/Ω_c as determined by Eq. (24) for the experimental parameters $\Omega_c/\omega_z = 6.62$. Here R_B is the radius at the Brillouin condition, $\omega/\Omega_c = 1/2$, which yields the minimum radius and maximum density. The points are experimental measurements, and one can see that the agreement with theory is very good.

To understand the plasma evolution along the curve, we

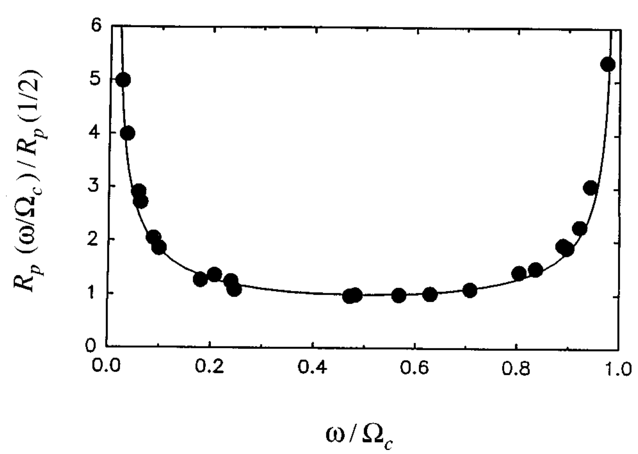

FIG. 5. Radius R_p of a spheroidal 2000 $^9Be^+$ ion plasma as a function of rotation frequency. The radius is scaled to the radius at the Brillouin limit and the rotation frequency to the cyclotron frequency. The solid curve is the theoretical prediction with no adjustable parameters. Taken from Ref. 2.

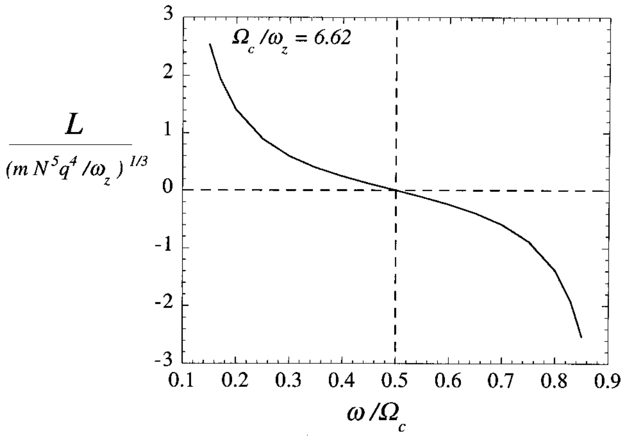

FIG. 6. Scaled angular momentum as a function of ω/Ω_c, calculated for the trap parameters that correspond to the experimental results illustrated in Fig. 5.

obtain an expression for the angular momentum as a function of ω. In general the total canonical angular momentum for a thermal equilibrium plasma is given by

$$L=m\left(\frac{\Omega_c}{2}-\omega\right)\int 2\pi r\ dr\ dz\ n(r,z)r^2, \tag{26}$$

where use has been made of the fact that the velocity dependence of f_c is a product of Maxwellians in a frame that rotates with frequency $-\omega$. For a uniform density spheroid, this reduces to

$$L^{(0)}=Nm\Omega_v R_p^2/5, \tag{27}$$

where the superscript zero has been added to note that this expression refers to the limit of a zero thickness surface sheath. Corrections due to the surface sheath will be obtained in Sec. IV. In Fig. 6 the scaled angular momentum,

$$\frac{L^{(0)}}{(mN^5e^4/\omega_z)^{1/3}}=\frac{\Omega_v}{5\omega_z}\left[\frac{3}{(2\beta+I)\alpha(\beta)}\right]^{2/3}, \tag{28}$$

is plotted versus ω/Ω_c for the experimental parameters $\Omega_c/\omega_z=6.62$. Here use has been made of Eq. (24).

In the experiment, the torque laser exerted a negative torque, that is, a torque in the same sense as the plasma rotation. The plasma started off in a state with large and positive L and, correspondingly, with small rotation frequency, density, and aspect ratio (i.e., $\omega\simeq\omega_m$, $\omega_p\simeq\omega_z$, and $\alpha\simeq 0$). As L was decreased, the rotation frequency, density, and aspect ratio all increased. When L passed through zero, the rotation frequency was $\omega=\Omega_c/2$ and the density and aspect ratio reached their maximum values [$\omega_p=\Omega_c/\sqrt{2}$ and $\alpha=g^{-1}(2\omega_z^2/\Omega_c^2)$]. As L became progressively more negative, the frequency continued to increase, but the density and aspect ratio decreased. For large and negative L, the frequency approached the upper limit $\Omega_c-\omega_m$, and the density and aspect ratio again approached their minimum values ($\omega_p=\omega_z$ and $\alpha\simeq 0$).

One may worry that we did not explicitly specify the value of E in determining the plasma state; Eq. (28) determines ω as a function of trap parameters and the values of L and N. However, this whole analysis implicitly assumes that the cooling laser continually adjusts the value of E so that T (and λ_D) remain small (formally zero).

Also, the analysis assumes that the evolution is sufficiently slow that the plasma passes through a sequence of thermal equilibrium states. This is the kind of transport that we want to describe more generally using a thermodynamic approach. To that end, we first develop a thermodynamic formalism for the trapped plasmas.

IV. THERMODYNAMIC FRAMEWORK

A modern development of thermodynamics starts from the definition of the free energy

$$F_R(T,\omega,B,\{V_j\},N)=-kT\ \ln Z_c \tag{29}$$

in terms of the canonical partition function

$$Z_c=\frac{1}{N!(h/m)^{3N}}\int d^3\mathbf{r}_1\cdots d^3\mathbf{v}_N\ \exp[-(H+\omega P_\theta)/kT], \tag{30}$$

where h is Planck's constant.[19] Here the subscript R is a reminder that F_R is the free energy in the rotating frame of the plasma. The quantities $(T,\omega,B,\{V_j\},N)$ are a complete set of thermodynamic variables, since they determine the value of Z_c. The trap geometry is assumed to be given and fixed. The dependence on T, ω, and N is obvious, the dependence on B enters through P_θ, and the dependence on V_j (the potential on the jth electrode) enters through H. Although $(T,\omega,B,\{V_j\},N)$ are a complete set of thermodynamic variables, they are not the only complete set.

Other thermodynamic variables are introduced as partial derivatives of F_R. For example, from Eqs. (29) and (30) it follows that

$$-T^2\frac{\partial}{\partial T}\left[\frac{F_R}{T}\right]_{\omega,B,\{V_j\},N}=\langle H_R\rangle\equiv E_R, \tag{31}$$

where the bracket indicates an average over the Gibbs distribution. The entropy S is defined through the relation

$$F_R=E_R-TS, \tag{32}$$

which together with Eq. (31) implies the familiar result

$$\left.\frac{\partial F_R}{\partial T}\right)_{\omega,B,\{V_j\},N}=-S. \tag{33}$$

Likewise, the partial derivatives of F_R with respect to the other thermodynamic variables are physically meaningful quantities. For example, the partial derivative with respect to ω yields the angular momentum

$$\left.\frac{\partial F_R}{\partial \omega}\right)_{T,B,\{V_j\},N}=\langle P_\theta\rangle\equiv L, \tag{34}$$

and the partial derivative with respect to N is by definition the chemical potential

$$\left.\frac{\partial F_R}{\partial N}\right)_{T,\omega,B,\{V_j\}}=\mu. \tag{35}$$

This function plays an important role in determining the thermal equilibrium of systems in which the number of particles can fluctuate.

The partial derivative of F_R with respect to B is equal to the average magnetic moment of the plasma

$$\left.\frac{\partial F_R}{\partial B}\right)_{T,\omega,\{V_j\},N}=\int d^3\mathbf{r}_1\cdots d^3\mathbf{v}_N\,\frac{e}{2c}\,\omega\sum_{i=1}^{N} r_i^2 f_c(\mathbf{r}_1,\ldots,\mathbf{v}_N)$$
$$=\frac{Ne}{2c}\,\omega\langle r^2\rangle=-M, \tag{36}$$

where the minus sign enters the last equality because $-\omega$ is the rotation frequency of the plasma. Note that M is a negative quantity for a non-neutral plasma, indicating that the magnetization induced by rotation opposes the applied magnetic field: the plasma is diamagnetic. This appears to contradict the Bohr–van-Leeuwen theorem, which states that classical systems cannot display diamagnetism.[30] However, the theorem only applies to systems which do not rotate in thermal equilibrium. In a non neutral plasma the magnetic moment arises from the current created by rotation.

The partial derivative of F_R with respect to the electrode voltage V_j is equal to the average charge q_j induced on the electrode by the plasma:

$$\left.\frac{\partial F_R}{\partial V_j}\right)_{T,\omega,B,\{V_{k\neq j}\},N}=-q_j\,. \tag{37}$$

To prove this relation we note that the voltages V_j enter the Hamiltonian H_R only through the trap potential $\phi_T(\mathbf{r})$, whose linear dependence on $\{V_j\}$ can be expressed as

$$\phi_T(\mathbf{r})=\sum_j V_j\hat{\phi}_T^{(j)}(\mathbf{r}), \tag{38}$$

where $\hat{\phi}_T^{(j)}(\mathbf{r})$ is the potential caused by a unit voltage on electrode (j). Then Eqs. (9), (29), and (30) imply that

$$\left.\frac{\partial F_R}{\partial V_j}\right)_{T,\omega,B,N,\{V_{k\neq j}\}}$$
$$=\int d^3\mathbf{r}_1\cdots d^3\mathbf{v}_N\sum_i e\hat{\phi}_T^{(j)}(\mathbf{r}_i)f_c(\mathbf{r}_1,\cdots,\mathbf{v}_N)$$
$$=\sum_i\langle e\hat{\phi}_T^{(j)}(\mathbf{r}_i)\rangle. \tag{39}$$

This average can be related to q_j by using Poisson's equation for the electrostatic potential ϕ induced by the N charges in the plasma:

$$\nabla^2\phi=-\sum_i 4\pi e\,\delta(\mathbf{r}-\mathbf{r}_i), \tag{40}$$

with the boundary condition that $\phi=0$ on the electrodes. Multiplying each side by $\hat{\phi}_T^{(j)}(\mathbf{r})$ and integrating over $\mathbf{r}$ implies

$$\int d^3\mathbf{r}[\hat{\phi}_T^{(j)}(\mathbf{r})\nabla^2\phi]=-\sum_i 4\pi e\hat{\phi}_T^{(j)}(\mathbf{r}_i). \tag{41}$$

Now we add $-\phi(\mathbf{r})\nabla^2\hat{\phi}_T^{(j)}$ to the integrand on the left-hand side, which makes no change since $\nabla^2\hat{\phi}_T^{(j)}=0$ except on the wall where $\phi=0$. However, this allows us to apply Green's theorem:

$$\int d^3\mathbf{r}[\hat{\phi}_T^{(j)}\nabla^2\phi-\phi\nabla^2\hat{\phi}_T^{(j)}]$$
$$=\int d\mathbf{S}\cdot[\hat{\phi}_T^{(j)}\nabla\phi-\phi\nabla\hat{\phi}_T^{(j)}], \tag{42}$$

where the surface integral runs over the electrodes. However, on the electrodes $\phi=0$, and $\hat{\phi}_T^{(j)}$ equals 1 on electrode j and equals 0 on the other electrodes, so we have

$$\int_{s_j} d\mathbf{S}\cdot\nabla\phi=-\sum_i 4\pi e\hat{\phi}_T^{(j)}(\mathbf{r}_i), \tag{43}$$

where the surface integral runs only over electrode j. Taking the average of this equation and using the relation $\int_{s_j}d\mathbf{S}\cdot\nabla\phi=4\pi q_j$, yields Eq. (37).

The partial derivatives of the free energy expressed in Eqs. (33)–(37) can be summarized by the total differential

$$dF_R=-SdT+Ld\omega-\sum_j q_j dV_j-M\;dB+\mu dN. \tag{44}$$

F_R is an example of a thermodynamic potential for the system. By making Legendre transformations, we obtain the total differential of other thermodynamic potentials.[19] For example, using Legendre transformation (32) to eliminate F_R in favor of E_R yields the total differential

$$dE_R=T\;dS+Ld\omega-\sum_j q_j dV_j-M\;dB+\mu dN. \tag{45}$$

Likewise, using the Legendre transformation $E=E_R-\omega L$ to exchange E_R for the energy in the laboratory frame E [see Eq. (6)] yields

$$dE=T\;dS-\omega dL-\sum_j q_j dV_j-M\;dB+\mu dN. \tag{46}$$

Obviously, this procedure can be continued to generate many such total differentials.

Simply by rearranging terms, Eqs. (45) and (46) can be rewritten in the traditional form $TdS=\cdots$. For many situations, the trap parameters and the particle number are constant (i.e., $dB=dV_j=dN=0$), so Eq. (46) reduces to the form

$$TdS=dE+\omega dL. \tag{47}$$

This equation is formally equivalent to the well-known TdS equation for a gas

$$TdS=dE+pdV, \tag{48}$$

where p corresponds to ω and V to L. We will make use of this formal correspondence from time to time as we proceed.

A. Maxwell relations

By taking cross derivatives of the coefficients in the total differentials, we obtain many Maxwell relations (hundreds). Simple examples that follow from Eq. (44) are the following:

$$\left.\frac{\partial L}{\partial T}\right)_{\omega,B,\{V_j\},N}=\frac{\partial^2 F_R}{\partial T\partial\omega}=-\left.\frac{\partial S}{\partial\omega}\right)_{T,B,\{V_j\},N}, \tag{49}$$

$$\left.\frac{\partial L}{\partial B}\right)_{T,\omega,\{V_j\},N}=\left.\frac{\partial^2 F_R}{\partial B\partial\omega}\right)=-\left.\frac{\partial M}{\partial\omega}\right)_{T,B,\{V_j\},N}, \tag{50}$$

$$\left.\frac{\partial q_j}{\partial V_k}\right)_{T,\omega,B,\{V_{l\neq k}\},N}=-\frac{\partial^2 F_R}{\partial V_k\partial V_j}=\left.\frac{\partial q_k}{\partial V_j}\right)_{\omega,T,B,\{V_{l\neq j}\},N}. \tag{51}$$

Equations (49) and (50) are typical of Maxwell relations in that they connect quantities that at first glance seem unrelated. Of course, the relations are general. Equation (51) might seem to be a simple reciprocal relation from electrostatics but, in fact, is more general since it involves the plasma response.

It is convenient to work theoretically with the variables T and ω since these variables enter the Gibbs distribution explicitly. However, these may not be the easiest variables to manipulate experimentally; E and L may be easier to control than T and ω. For example, it may be easier to calculate the specific heat at constant rotation frequency

$$c_\omega=T\left.\frac{\partial S}{\partial T}\right)_\omega \tag{52}$$

but easier to measure the specific heat at constant angular momentum

$$c_L=T\left.\frac{\partial S}{\partial T}\right)_L, \tag{53}$$

where B, $\{V_j\}$, and N are held constant in both cases. Fortunately, Maxwell relations (or combinations of Maxwell relations) provide general relations between such quantities.

Rather than develop these relations explicitly, we make use of the formal correspondence between the TdS equation for a gas and the TdS equation for a rotating plasma [see Eqs. (47) and (48)]. Recalling that ω corresponds to p and L to V, we see that c_L corresponds to the specific heat at constant volume c_v and c_ω to the specific heat a constant pressure c_p. Simply transcribing the well-known relation between c_v and c_p through the replacements $p\rightarrow\omega$ and $V\rightarrow L$ yields the relation[19]

$$c_\omega-c_L=-T\frac{(\partial L/\partial T)_\omega^2}{\partial L/\partial\omega)_T}. \tag{54}$$

In the next section, we will show that $\partial L/\partial\omega)_T\leqslant 0$ and that $c_L\geqslant 0$, so Eq. (54) implies that $c_\omega\geqslant c_L\geqslant 0$. Also, we will see that for a large plasma, the relative difference between c_ω and c_L vanishes.

Other useful general relations linking derivatives at constant T and ω to those at constant E and L can also be borrowed from the standard p-V system[19]

$$\left.\frac{\partial E}{\partial T}\right)_L=c_L, \tag{55}$$

$$\left.\frac{\partial E_R}{\partial T}\right)_\omega=c_\omega, \tag{56}$$

$$\left.\frac{\partial E}{\partial L}\right)_T=T\left.\frac{\partial\omega}{\partial T}\right)_L-\omega, \tag{57}$$

$$\left.\frac{\partial E}{\partial\omega}\right)_T=-T\left.\frac{\partial L}{\partial T}\right)_\omega-\omega\left.\frac{\partial L}{\partial\omega}\right)_T, \tag{58}$$

$$\left.\frac{\partial E}{\partial T}\right)_\omega=c_\omega-\omega\left.\frac{\partial L}{\partial T}\right)_\omega. \tag{59}$$

The properties of Jacobians can be used to relate the derivative of any quantity A at fixed E to a derivative at fixed T. For example,[19]

$$\begin{aligned}\left.\frac{\partial A}{\partial B}\right)_E&=\frac{\partial(A,E)}{\partial(B,E)}=\frac{\partial(A,E)/\partial(A,T)\,\partial(A,T)/\partial(B,T)}{\partial(B,E)/\partial(B,T)}\\&=\left.\frac{\partial A}{\partial B}\right)_T\frac{\partial E/\partial T)_A}{\partial E/\partial T)_B}.\end{aligned} \tag{60}$$

A similar relation between derivatives at fixed L and fixed ω can be derived by substituting L for E and ω for T in Eq. (60). Finally, the Jacobian of the transformation from (E,L) to (T,ω) can be written as

$$\frac{\partial(E,L)}{\partial(T,\omega)}=\left.\frac{\partial L}{\partial\omega}\right)_T c_L. \tag{61}$$

B. Thermodynamic inequalities

The stability of a system in thermal equilibrium against fluctuations away from equilibrium provides several useful inequalities.[19] We begin the derivation of these inequalities by defining the system energy $E'=E+\Sigma_j q_j V_j+MB$, which differs from the plasma (or particle) energy $E=\langle H\rangle$ through the addition of the energy associated with the induced image charges and the plasma magnetic moment. E' is the total work, including that done by external circuits, required to construct a plasma out of individual charges brought in from infinity to a trap with fixed electrode voltages V_j and fixed current in the solenoid that is used to maintain the magnetic field B. Here, as elsewhere in the paper, B is the uniform vacuum field, so constant current is equivalent to constant B. Note that M is small and that terms of order M^2 were neglected in $E=\langle H\rangle$, when diamagnetic interactions (and relativistic corrections) were omitted in writing Hamiltonian (2). The analysis should be thought of as an expansion carried only to first order in M. As the plasma is assembled in the trap, image charges q_j run onto the electrodes and the voltage sources for the electrodes do work $\Sigma_j q_j V_j$. Likewise the current source does work MB, the energy associated with mutual inductance between the plasma and the surrounding solenoid. For future reference, we write the TdS equation following from Eq. (46) in terms of E' rather than E:

$$dE'=TdS-\omega dL+\sum_j V_j dq_j+BdM+\mu dN. \tag{62}$$

We consider a plasma that is confined in a trap with fixed electrode voltages $V_j = V_{j0}$, fixed magnetic field $B = B_0$, and is in contact with a heat, angular momentum, and particle reservoir parametrized by temperature T_0, rotation frequency $-\omega_0$, and chemical potential μ_0. Initially, we postulate that the system is slightly out of equilibrium; it does not have the values of E, L, q_j, M, or N that would correspond to $(T_0, \omega_0, V_{j0}, B_0, \mu_0)$ in thermal equilibrium. The system adjusts itself by interacting with the reservoir, exchanging energy, angular momentum and particles, and by also interacting with the external circuits that fix the electrode voltages and magnetic field. In what follows these circuits are assumed to have no entropy associated with them, and the plasma and heat reservoir constitute a thermally isolated system (no heat is exchanged with the circuits, but work may be done on them). For example, a constant voltage can be maintained by a homopolar generator that consists of a massive conducting flywheel that rotates through a transverse magnetic field. The state of the wheel is described by a single degree of freedom, the rotation angle, so there is negligible entropy.

The second law then implies that the total entropy of the plasma and the reservoir must be non-negative in this equilibration process:

$$\Delta S + \Delta S_{\text{res}} \geqslant 0. \tag{63}$$

Furthermore, the entropy change of the reservoir is related to the heat Q absorbed into the system from the reservoir,

$$\Delta S_{\text{res}} = \frac{-Q}{T_0}. \tag{64}$$

However, the first law for the plasma states that

$$Q = \Delta E' + W, \tag{65}$$

where $\Delta E'$ is the change in energy of the system (including the energy of image charges and the magnetic energy associated with M), and W is the work done by this system. The system can do work as it comes to equilibrium in a number of ways: for instance, induced image charges can flow onto or off of the electrodes, which requires the system to do work $-\Sigma_j V_{0j} \Delta q_j$ against the circuits that hold the electrode voltages fixed; angular momentum and particle exchange with the reservoir causes work $\omega_0 \Delta L - \mu_0 \Delta N$ to be performed; and a change in magnetic moment ΔM of the plasma does work $-B_0 \Delta M$ against the power supply that fixes the current in the magnetic field solenoid. Adding these contributions yields the relation

$$W = \omega_0 \Delta L - \sum_j V_{0j} \Delta q_j - B_0 \Delta M - \mu_0 \Delta N. \tag{66}$$

This relation can also be obtained directly from Eq. (62) by considering the change in E' at constant entropy, and setting $W = -\Delta E'$.

Substitution of Eqs. (64)–(66) into Eq. (63), and then multiplication by the negative constant $-T_0$ implies

$$\Delta \Omega_R \leqslant 0, \tag{67}$$

where

$$\Omega_R \equiv E' - T_0 S + \omega_0 L - \sum_j V_{0j} q_j - B_0 M - \mu_0 N \tag{68}$$

is a thermodynamic potential for the plasma. When $\omega = \omega_0$, $V_j = V_{0j}$, and $B = B_0$, $\Omega_R = E_R - T_0 S - \mu_0 N$ is the grand potential[19] of the plasma as seen in a rotating frame. From Eq. (67) we conclude that the thermal equilibrium state achieved by a non neutral plasma connected to a heat, angular momentum and particle reservoir and confined by constant electrode voltages and constant external magnetic field is the state for which the thermodynamic potential Ω_R is minimized.

Let us now examine the consequences of this result by considering small fluctuations of the system away from thermal equilibrium to some nearby state, under the conditions that T_0, ω_0, V_{0j}, B_0, and μ_0 are fixed. Since the system started in thermal equilibrium the thermodynamic potential Ω_R must increase away from equilibrium, and we can use this fact to determine thermodynamic inequalities. Say that there are P electrodes. Then let $\{\lambda_k\}$, $k = 1,...,P+4$, be any complete set from the $P+4$ conjugate pairs of thermodynamic variables

$$\{(T,S),(-\omega,L),\{(V_j,q_j)\},(B,M),(\mu,N)\}. \tag{69}$$

Note that $-\omega$, the rotation frequency of the plasma, is the variable conjugate to the plasma angular momentum. The term "conjugate" is used here in the sense that conjugate pairs are connected by a derivative of the system energy [see Eq. (62)].

The nearby state to which the system has been perturbed is assumed to be characterized by changes in the λ_k's by small amounts $\delta\lambda_k$. The change in Ω_R compared to the minimum equilibrium value is then

$$\delta\Omega_R = \sum_k \frac{\partial \Omega_R}{\partial \lambda_k} \delta\lambda_k + \frac{1}{2} \sum_{j,k} \frac{\partial^2 \Omega_R}{\partial \lambda_j \partial \lambda_k} \delta\lambda_j \delta\lambda_k \geqslant 0, \tag{70}$$

where the inequality follows from the fact that Ω_R is minimized in the thermal equilibrium for which $\delta\lambda_k = 0$.

Now since $\delta\lambda_k$ can be either positive or negative, the first variation of Ω_R must vanish, implying

$$\frac{\partial \Omega_R}{\partial \lambda_k} = 0. \tag{71}$$

By using the definition of Ω_R in Eq. (68) and substituting for $\partial E'/\partial \lambda_j$ from Eq. (62), we can rewrite Eq. (71) as

$$\frac{\partial \Omega_R}{\partial \lambda_k} \doteq (T - T_0) \frac{\partial S}{\partial \lambda_k} - (\omega - \omega_0) \frac{\partial L}{\partial \lambda_k} + \sum_j (V_j - V_{0j}) \frac{\partial q_j}{\partial \lambda_k} + (B - B_0) \frac{\partial M}{\partial \lambda_k} + (\mu - \mu_0) \frac{\partial N}{\delta \lambda_k} = 0. \tag{72}$$

This equation implies that the thermal equilibrium state is such that

$$T = T_0, \quad \omega = \omega_0, \quad V_j = V_{j0}, \quad B = B_0, \quad \text{and} \quad \mu = \mu_0. \tag{73}$$

For example, suppose that $\{\lambda_k\} = \{S, L, \{q_j\}, M, N\}$ and that

$\lambda_k = S$. Then in Eq. (72), $\partial S/\partial\lambda_k$ is unity and the remaining partial derivatives are zero, so we obtain $T = T_0$. The other results in Eq. (73) follow from setting $\lambda_k = L$, $\{q_j\}$, M, and N one after the other.

When conditions (73) are satisfied, only the term quadratic in the $\delta\lambda_k$'s survives and inequality (67) implies that this term must be non-negative. In other words, in the space of $\{\delta\lambda_k\}$ the surfaces of constant $\delta\Omega_R$ are closed and nested so that $\delta\Omega_R = 0$ is a local minimum. Since this is a statement concerning the topology of the constant $\delta\Omega_R$ surfaces, it remains true for any complete set of λ_k's that we choose. Therefore we lose no information by choosing any particular set of λ_k's. A convenient set is $\{\lambda_k\} = \{S, L, \{q_j\}, M, N\}$, because we have already determined the first derivatives of Ω_R with respect to these variables [see Eq. (72)]. For example, $\partial^2\Omega_R/\partial S^2)_{L,\{q_j\},M,N} = \partial T/\partial S)_{L,\{q_j\},M,N}$. The entire set of second derivatives forms a matrix of dimensions $P+4$ by $P+4$:

$$\frac{\partial^2\Omega_R}{\partial\lambda_j\partial\lambda_k} = \begin{pmatrix} \left.\frac{\partial T}{\partial S}\right)_{L,\{q_j\},M,N} & \left.\frac{\partial T}{\partial L}\right)_{S,\{q_j\},M,N} & \left\{\left.\frac{\partial T}{\partial q_k}\right)_{S,L,\{q_{j\neq 1}\},M,N}\right\} & \left.\frac{\partial T}{\partial M}\right)_{S,L,\{q_j\},N} & \left.\frac{\partial T}{\partial N}\right)_{S,L,\{q_j\},M} \\ & -\left.\frac{\partial \omega}{\partial L}\right)_{S,\{q_j\},M,N} & \left\{-\left.\frac{\partial \omega}{\partial q_k}\right)_{S,L,\{q_{j\neq k}\},M,N}\right\} & -\left.\frac{\partial \omega}{\partial M}\right)_{S,L,\{q_j\},N} & -\left.\frac{\partial \omega}{\partial N}\right)_{S,L,\{q_j\},M} \\ & & \left\{\left.\frac{\partial V_j}{\partial q_k}\right)_{S,L,\{q_{j\neq k}\},M,N}\right\} & \left.\frac{\partial V_j}{\partial M}\right)_{S,L,\{q_j\},N} & \left.\frac{\partial V_j}{\partial N}\right)_{S,L,\{q_j\},M} \\ \cdots & & & \left.\frac{\partial B}{\partial M}\right)_{S,L,\{q_j\},N} & \left.\frac{\partial B}{\partial N}\right)_{S,L,\{q_j\},M} \\ & & & & \left.\frac{\partial u}{\partial N}\right)_{S,L,\{q_j\},M} \end{pmatrix}, \tag{74}$$

where only the top half of the matrix is displayed because it is symmetric: $\partial^2\Omega_R/\partial\lambda_j\partial\lambda_k = \partial^2\Omega_R/\partial\lambda_k\partial\lambda_j$. (This symmetry provides a set of Maxwell relations for the system.)

Stability implies that the eigenvalues of this matrix are non-negative, which yields $P+4$ thermodynamic inequalities. These inequalities form a necessary and sufficient set of criteria for stability of the equilibrium against fluctuations in any of the thermodynamic variables.

However, the eigenvalues are quite complicated in form, so we consider a simpler set of inequalities, which only form a necessary set of criteria for stability (they are not sufficient). Considering fluctuations in only one of the λ_k's at a time implies that each diagonal element, $\partial^2\Omega_R/\partial\lambda_k^2$, must be non-negative. For example, we find

$$\partial T/\partial S)_{L,\{q_j\},M,N} \geqslant 0, \tag{75}$$

which implies that the specific heat at constant L, $\{q_j\}$, M, and N is non-negative, provided that $T \geqslant 0$. It is also worthwhile to write out the other inequalities explicitly:

$$-\left.\frac{\partial\omega}{\partial L}\right)_{S,\{q_j\},M,N} \geqslant 0, \tag{76}$$

$$\left.\frac{\partial V_k}{\partial q_k}\right)_{S,L,\{q_{j\neq k}\},M,N} \geqslant 0, \tag{77}$$

$$\left.\frac{\partial B}{\partial M}\right)_{S,L,\{q_j\},N} \geqslant 0, \tag{78}$$

$$\left.\frac{\partial \mu}{\partial N}\right)_{S,L,\{q_j\},M} \geqslant 0. \tag{79}$$

The fact that these inequalities are necessary but not sufficient for stability can be seen by allowing variations in more than one parameter. For example, consider variations in both S and L. Then the determinant of the 2×2 matrix composed of the upper left-hand side of $\partial^2\Omega_R/\partial\lambda_j\partial\lambda_k$ must be non-negative, which implies that

$$-\left(\left.\frac{\partial T}{\partial S}\right)_{L,\{q_j\},M,N}\left.\frac{\partial\omega}{\partial L}\right)_{S,\{q_j\},M,N}\right) \geqslant \left(\left.\frac{\partial T}{\partial L}\right)_{S,\{q_j\},M,N}\right)^2, \tag{80}$$

providing more stringent bounds for both $\partial T/\partial S$ and $\partial\omega/\partial L$ than are provided by Eqs. (75) and (76).

Equations (75)–(79) reflect stability along one particular set of directions, given by $\{\lambda_k\} = \{S, L, \{q_j\}, M, N\}$, but more information may be uncovered by considering other directions. The inequalities so obtained take the simplest forms when only one of each conjugate pair in Eq. (69) is employed as a λ_k. For example, choose $\{\lambda_k\} = \{T, L, \{V_j\}, B, N\}$, and take $\lambda_k = L$ in Eq. (72). Then taking another derivative with respect to L yields

$$\left.\frac{\partial^2\Omega_R}{\partial L^2}\right)_{T,\{V_j\},B,N} = -\left.\frac{\partial\omega}{\partial L}\right)_{T,\{V_j\},B,N} \geqslant 0, \tag{81}$$

where we have employed the equilibrium conditions, Eq. (73), after taking the derivative. Figure 6 illustrates this inequality for the special case of a small cold ($\lambda_D \simeq 0$) plasma in a quadratic trap potential. Likewise, taking $\lambda_k = T$ in Eq. (72) yields $\partial S/\partial T)_{L,\{V_j\},B,N} \geqslant 0$. Assuming that $T > 0$, and using definition (55), we find that the specific heat c_L must be non-negative. This fact together with Eq. (54) implies that $c_\omega \geqslant 0$ as well. Analogous arguments show that any other choice for the set of $\{\lambda_k\}$'s consisting of one variable from each of the conjugate pairs in Eq. (69) can be employed without changing the basic form of Eqs. (75)–(79). For example, $\partial M/\partial B)_{T,\omega,\{V_j\},N} \geqslant 0$ and $\partial V_j/\partial q_j)_{T,L,\{V_{k\neq j}\},B,\mu} \geqslant 0$ as well.

The inequalities $c_L \geqslant 0$ and $\partial\omega/\partial L)_T \leqslant 0$ are the analogs of the inequalities $c_v \geqslant 0$ and $\partial p/\partial V)_T \leqslant 0$ for a gas. The latter two inequalities can be understood physically as the conditions for temperature and mechanical stability when the gas is in contact with a reservoir characterized by fixed temperature and pressure. Likewise, the inequalities $c_\omega \geqslant 0$ and $\partial\omega/\partial L)_T \leqslant 0$ are necessary for temperature and rotation frequency stability when the plasma is in contact with a reservoir characterized by fixed temperature and fixed rotation frequency. In thinking about frequency stability, it is necessary to remember that $-\omega$ is the rotation frequency, so it may be useful to rewrite $\partial\omega/\partial L)_T \leqslant 0$ as $\partial(-\omega)/\partial L)_T \geqslant 0$. Suppose, for example, that a fluctuation makes $-\omega$ larger (more positive) than the rotation frequency of the reservoir. The reservoir will then exert a negative torque on the plasma, opposing the differential rotation. The two inequalities $\Delta L < 0$ and $\partial(-\omega)/\partial L)_T > 0$ then imply that $\Delta(-\omega) < 0$, which is a frequency change of the sign required to restore equilibrium.

The inequality $\partial V_j/\partial q_j)_{T,L,\{V_{k\neq j}\},B,\mu} \geqslant 0$ also follows from a straightforward physical picture. As V_j is increased (holding the other parameters fixed), a plasma consisting of positive charges is pushed away from electrode j, so the (negative) image charge on that electrode is decreased in magnitude.

The inequality $\partial M/\partial B)_{T,\omega,\{V_j\},N} \geqslant 0$ implies that the magnitude of the plasma's (negative) magnetic moment M decreases as B increases, which may be counterintuitive at first glance since one expects the magnitude of the plasma magnetization to increase as B increases. In fact, the magnetization does tend to increase as B increases. However, the average magnetization is the magnetic moment divided by the plasma volume, and as B increases the plasma volume decreases since the plasma radius tends to shrink. It is the decrease in plasma volume which allows the magnetization to increase in magnitude even though the magnetic moment decreases in magnitude.

Finally, we may like to fix E rather than S or T. For example, consider variations of L at fixed E, V_j, B, and N. Taking $\lambda_k = L$ in Eq. (72), and then taking another derivative with respect to L yields the inequality

$$\left.\frac{\partial^2\Omega_R}{\partial L^2}\right)_{E,\{V_j\},B,N} = \left.\frac{\partial T}{\partial L}\right)_{E,\{V_j\},B,N} \left.\frac{\partial S}{\partial L}\right)_{E,\{V_j\},B,N} - \left.\frac{\partial\omega}{\partial L}\right)_{E,\{V_j\},B,N} \geqslant 0. \tag{82}$$

However, Eq. (46) implies that $T\partial S/\partial L)_{E,\{V_j\},B,N} = \omega$, so we can write Eq. (82) as

$$-T\,\frac{\partial}{\partial L}\left.\left(\frac{\omega}{T}\right)\right)_{E,\{V_j\},B,N} \geqslant 0. \tag{83}$$

C. Fluctuations

The thermodynamic inequalities discussed in the previous section can be related to the magnitude of fluctuations in the plasma, and some of these relations may be of physical interest. For example, consider a fluctuation $\delta q_i = q_i - \langle q_i\rangle$ in the charge on a sector i at fixed N, ω, T, B, and $\{V_j\}$. Here we employ the notation $\langle q_i\rangle$ for the equilibrium average, and q_i is the value of a particular realization of the canonical ensemble, which fluctuates by δq_i about $\langle q_i\rangle$. Standard thermodynamic arguments[19] allow us to express the average $\langle\delta q_i\delta q_j\rangle_{T,\omega}$ in terms of thermodynamic derivatives. We first express this average in terms of $\langle q_i q_j\rangle_{T,\omega}$, $\langle q_i\rangle$, and $\langle q_j\rangle$:

$$\langle\delta q_i\delta q_j\rangle_{T,\omega} = \langle q_i q_j\rangle_{T,\omega} - \langle q_i\rangle\langle q_j\rangle. \tag{84}$$

These averages can be expressed as derivatives of the canonical partition function Z_c. Using Eqs. (29), (30), and (37), one finds

$$\langle q_i\rangle = (kT/Z_c)\partial Z_c/\partial V_j)_{T,\omega,B,N}, \tag{85}$$

and a modification of the argument that led to Eq. (37) yields $\langle q_i q_j\rangle_{T,\omega} = [(kT)^2/Z_c]\partial^2 Z_c/\partial V_i\partial V_j)_{T,\omega,B,N}$. Putting these averages together in Eq. (84) yields

$$\begin{aligned}\langle\delta q_i\delta q_j\rangle_{T,\omega} &= \frac{1}{Z_c}\,(kT)^2\left.\frac{\partial^2}{\partial V_i\partial V_j}\,Z_c\right)_{T,\omega} - \left(\frac{kT}{Z_c}\right)^2\frac{\partial Z_c}{\partial V_i}\,\frac{\partial Z_c}{\partial V_j}\\ &= (kT)^2\left.\frac{\partial^2 \ln Z_c}{\partial V_i\partial V_j}\right)_{T,\omega,B,N}\\ &= kT\left.\frac{\partial q_i}{\partial V_j}\right)_{T,\omega,B,N} = kT\left.\frac{\partial q_j}{\partial V_i}\right)_{T,\omega,B,N},\end{aligned} \tag{86}$$

where in the last two steps we used Eq. (85) and Maxwell's relation, (51). The subscripts on $\langle\delta q_i\delta q_j\rangle_{T,\omega}$ point out that the average is performed in a constant T and ω ensemble (the canonical ensemble). Averages over the microcanonical ensemble will be discussed presently.

When $i=j$ the fact that $\langle\delta q_i^2\rangle_{T,\omega}$ must be non-negative provides us with an inequality similar to Eq. (77). Furthermore, fluctuations in image charge may be of some interest since Eq. (86) shows that they provide a measure of the temperature of the plasma. A similar relation can be derived involving the magnetic moment M of the plasma:

$$\langle\delta M^2\rangle_{T,\omega} = kT\left.\frac{\partial M}{\partial B}\right)_{T,\omega,\{V_j\},N}, \tag{87}$$

which provides us with an inequality similar to that given by Eq. (78). Measurements of fluctuations in M, through the use of a circuit connected to an external inductance coupled to the plasma, for example, could also provide a temperature diagnostic.

Another useful relation follows from consideration of fluctuations in the function $(1/N)\ \Sigma_i r_i^2$. The thermal equilibrium average of this function is the mean-square cylindrical radius, $\langle r^2\rangle$, and this average can be obtained by taking a derivative of the free energy with respect to ω:

$$\langle r^2\rangle = \frac{2}{Nm\Omega_v}\left.\frac{\partial F_R}{\partial\omega}\right)_{T,\{V_j\},B,N}. \tag{88}$$

Fluctuations in $(1/N)\Sigma_i r_i^2$ can be related to a derivative of $\langle r^2\rangle$ using arguments analogous to those that led to Eq. (86):

$$\left\langle\left(\delta\frac{1}{N}\sum_i r_i^2\right)^2\right\rangle_{T,\omega} = -\frac{2kT}{Nm\Omega_v}\left.\frac{\partial\langle r^2\rangle}{\partial\omega}\right)_{T,\{V_j\},B,N}. \tag{89}$$

This relation implies that

$$\frac{T}{\Omega_v}\left.\frac{\partial\langle r^2\rangle}{\partial\omega}\right)_{T,\{V_j\},B,N} \leqslant 0. \tag{90}$$

When Ω_v is positive, the mean-square radius shrinks as ω increases, but when Ω_v becomes negative $\langle r^2\rangle$ expands. Figure 5 illustrates this dependence for the special case of a quadratic trap potential.

Equation (90) can be employed to obtain an improved bound on $\partial L/\partial\omega$. By recalling that the velocity dependence in f_c is a product of Maxwellians in a frame that rotates with frequency $-\omega$, we obtain

$$L = m(\Omega_v/2)N\langle r^2\rangle. \tag{91}$$

A derivative with respect to ω implies the relation

$$\frac{Nm}{2}\,\Omega_v\left.\frac{\partial\langle r^2\rangle}{\partial\omega}\right)_{T,\{V_j\},B,N} = \left.\frac{\partial L}{\partial\omega}\right)_{T,\{V_j\},B,N} + Nm\langle r^2\rangle. \tag{92}$$

Since Eq. (90) implies that the left-hand side of Eq. (92) is less than or equal to zero, we find the inequality

$$\left.\frac{\partial L}{\partial\omega}\right)_{T,\{V_j\},B,N} \leqslant -Nm\langle r^2\rangle, \tag{93}$$

which is an improvement over inequality (76). Note that the right-hand side of Eq. (93) is the negative of the rotational inertia of the plasma. Equation (93) again points out that Eqs. (75)–(79) are necessary but not sufficient conditions for a stable equilibrium.

It is important to point out that the fluctuations in Eqs. (86), (87), and (89) are assumed to occur in a system at fixed ω and T. We have added subscripts to the averages in order to point this out explicitly. However, it is presumably fluctuations at fixed L and E that are of interest in many experimental measurements. Although we have said that averages in the microcanonical (fixed L and E) and canonical (fixed ω and T) ensembles are identical for large systems, this statement must be modified when fluctuations are considered. A more precise statement is that averages of intensive quantities in the two ensembles are identical to $O(1/N)$. However, for fluctuations these $O(1/N)$ corrections are important, and the two ensembles may provide different results in the thermodynamic limit. One trivial example is that in the microcanonical ensemble $\langle\delta P_\theta^2\rangle_{E,L}=0$, whereas in the canonical ensemble P_θ fluctuates. The reason that the $O(1/N)$ corrections are important can be understood from the following argument. Consider the fluctuation δA of an extensive quantity A. We evaluate $\langle\delta A^2\rangle$ by taking the difference $\langle\delta A^2\rangle = \langle A^2\rangle - \langle A\rangle^2$. Since A is extensive, $\langle A^2\rangle$ and $\langle A\rangle^2$ scale as N^2. The $O(1/N)$ difference between an evaluation of the averages using different ensembles will therefore scale as N. However, typical fluctuations $\langle\delta A^2\rangle$ are also of $O(N)$; the $O(N^2)$ terms cancel after $\langle A\rangle^2$ is subtracted from $\langle A^2\rangle$. We therefore cannot necessarily neglect the $O(1/N)$ difference between evaluations of rms fluctuations using different ensembles.

Fortunately, it is possible to relate the fluctuations in different ensembles.[31] Given any two quantities G and H with average values $\langle G\rangle$, $\langle H\rangle$ and fluctuations δG and δH about their average values, the fluctuations in a constant E, L, B, $\{V_j\}$, and N ensemble are related to the fluctuations in a constant T, ω, B, $\{V_j\}$, and N ensemble by

$$\begin{aligned}\langle\delta G\,\delta H\rangle_{E,L} &= \langle\delta G\,\delta H\rangle_{T,\omega} - kT^2\left.\frac{\partial T}{\partial E}\right)_L \left.\frac{\partial\langle G\rangle}{\partial T}\right)_{(\omega/T)} \\ &\quad\times\left.\frac{\partial\langle H\rangle}{\partial T}\right)_{(\omega/T)} + k\left.\frac{\partial T}{\partial L}\right)_E\left\{\left.\frac{\partial\langle G\rangle}{\partial T}\right)_{(\omega/T)}\left.\frac{\partial\langle H\rangle}{\partial(\omega/T)}\right)_T\right. \\ &\quad\left.+\left.\frac{\partial\langle G\rangle}{\partial(\omega/T)}\right)_T\left.\frac{\partial\langle H\rangle}{\partial T}\right)_{(\omega/T)}\right\} \\ &\quad+k\left.\frac{\partial(\omega/T)}{\partial L}\right)_E\left.\frac{\partial\langle G\rangle}{\partial(\omega/T)}\right)_T\left.\frac{\partial\langle H\rangle}{\partial(\omega/T)}\right)_T,\end{aligned} \tag{94}$$

where B, $\{V_j\}$, and N are also held fixed throughout. In Sec. V we will consider the case of a large trapped plasma and show that the mean-square fluctuations $\langle\delta q_i\delta q_j\rangle_{E,L}$ and $\langle\delta M^2\rangle_{E,L}$ are smaller than the fluctuations at constant T and ω, and are given by:

$$\langle\delta M^2\rangle_{E,L} = kT\left.\frac{\partial M}{\partial B}\right)_{T,L,\{V_j\},N}, \tag{95}$$

$$\langle\delta q_i\delta q_j\rangle_{E,L} = kT\left.\frac{\partial q_j}{\partial V_j}\right)_{T,L,B,N}. \tag{96}$$

These results differ from Eqs. (86) and (87) because L is held fixed in the derivatives, rather than ω.

Another example of a fluctuation for which there is a difference between ensembles in the large plasma limit is the rms fluctuation in the z component of the kinetic energy, $K_z=\Sigma_i \frac{1}{2}mv_z^2$. This quantity can be followed in computer simulations, and may also be observable using laser diagnostics in actual experiments, since these diagnostics can determine components of the particle velocities. In the canonical ensemble straightforward integrals over the Maxwellian velocity distribution imply that $\langle K_z\rangle = NkT/2$, so the measurement of $\langle K_z\rangle$ provides one with the temperature. Fluctuations in K_z are also related to T through averages over a Maxwellian:

$$\langle \delta K^2\rangle_{T,\omega}=\tfrac{1}{2}N(kT)^2. \tag{97}$$

However, using Eq. (94) one finds that in the constant E and L ensemble the mean-square fluctuation is different:

$$\langle \delta K_z^2\rangle_{E,L}=\frac{1}{2}\,N(kT)^2\left(1-\frac{Nk}{2c_L}\right). \tag{98}$$

There can be a considerable difference between Eqs. (97) and (98). For example, for a large weakly correlated electron plasma for which the cyclotron motion is quantized and in the ground state (but motion parallel to **B** remains classical), $c_L\rightarrow 1/2Nk$. Equation (98) then implies that $\langle \delta K_z^2\rangle_{E,L}$ vanishes. However, Eq. (97) implies that $\langle \delta K_z^2\rangle_{T,\omega}$ remains finite. In the microcanonical ensemble the fluctuation in K_z is nonzero only by virtue of correlations which raise c_L above $1/2Nk$.

D. Adiabatic processes

Some experiments involve adiabatic processes for which $S=$constant. For example, the rate of work done on the plasma due to different adiabatic processes is given by [see Eq. (46)]

$$\left.\frac{\partial E}{\partial V_j}\right)_{S,L,\{V_{k\neq j}\},B,N}=-q_j\,,\quad \left.\frac{\partial E}{\partial B}\right)_{S,L,\{V_j\},N}=-M,$$
$$\left.\frac{\partial E}{\partial L}\right)_{S,\{V_j\},B,N}=-\omega. \tag{99}$$

Typically, adiabatic expansions are carried out by varying a sector voltage V_j at constant L. The temperature change in such a process is

$$\left.\frac{\partial T}{\partial V_j}\right)_{S,L,\{V_{k\neq j}\},B,N}=-\,\partial S/\partial V_j)_{T,L,\{V_{k\neq j}\},B,N}/\partial S/\partial T)_{L,\{V_j\},B,N}$$
$$=-\frac{T}{c_L}\left.\frac{\partial q_j}{dT}\right)_{L,\{V_j\},B,N}, \tag{100}$$

where we have employed Eq. (53) and the Maxwell relation,

$$\left.\frac{\partial q_j}{\partial T}\right)_{L,B,\{V_k\},N}=-\frac{\partial(F_R-\omega L)}{\partial T\partial V_j}=\left.\frac{\partial S}{\partial V_j}\right)_{T,L,\{V_{k\neq j}\},B,N}. \tag{101}$$

Adiabatic expansions can also be carried out by varying the magnetic field. The temperature change would then be given by

$$\left.\frac{\partial T}{\partial B}\right)_{S,L,B,N}=-\frac{T}{c_L}\left.\frac{\partial M}{\partial T}\right)_{L,\{V_j\},B,N}. \tag{102}$$

V. THERMODYNAMIC FUNCTIONS FOR A LARGE TRAPPED PLASMA

As discussed in Sec. III B, large trapped plasmas have a uniform density out to some surface of revolution where the density falls to zero in a thin surface sheath. The uniform density is related to ω and Ω_c through Eq. (12). The interior of the trapped plasma is statistically equivalent (including all correlations) to an infinite homogeneous OCP. In this section, we relate the thermodynamic functions of a large trapped plasma to those of an OCP, which are well known.

We say that the trapped plasma is large when the thickness of the surface sheath λ is small compared to both the length and the radius of the plasma. The volume of the surface sheath is then small compared to the total plasma volume. As discussed in Sec. III B, λ is of order λ_D for a weakly correlated plasma and of order $\alpha n^{-1/3}$ for a strongly correlated plasma, where the factor α is near unity for a fluid state but can be a few tens for a crystal state.

A. Relation between energies

The first step in this program is to obtain a relation between the energies. The energy of a trapped plasma as viewed in the rotating frame is given by

$$E_R=\langle H_R\rangle=\frac{3}{2}\,NkT+\int d^3\mathbf{r}_1 e\,\phi_R(\mathbf{r}_1)n(\mathbf{r}_1)+\frac{N(N-1)}{2}$$
$$\times\int d^3\mathbf{r}_1 d^3\mathbf{r}_2 e^2 G(\mathbf{r}_1|\mathbf{r}_2)\rho^{(2)}(\mathbf{r}_1;\mathbf{r}_2), \tag{103}$$

where

$$\rho^{(2)}(\mathbf{r}_1,\mathbf{r}_2)=\int d^3\mathbf{v}_1\cdots d^3\mathbf{v}_N d^3\mathbf{r}_3\cdots d^3\mathbf{r}_N f_c \tag{104}$$

is the two-particle spatial distribution. In writing Eq. (103) we used the fact that the velocity dependence in f_c is a product of Maxwellians in the rotating frame. Setting

$$N(N-1)\rho(\mathbf{r}_1,\mathbf{r}_2)\simeq N^2\rho(\mathbf{r}_1,\mathbf{r}_2)$$
$$\equiv n(\mathbf{r}_1)n(\mathbf{r}_2)[1+g(\mathbf{r}_1,\mathbf{r}_2)], \tag{105}$$

where $g(\mathbf{r}_1,\mathbf{r}_2)$ is the spatial correlation function, yields the result

$$E_R=\frac{3}{2}NkT+\int d^3\mathbf{r}_1 n(\mathbf{r}_1)\bigg[e\,\phi_R(\mathbf{r}_1)$$
$$+\frac{1}{2}\int d^3r_2 e^2 G(\mathbf{r}_1|\mathbf{r}_2)n(\mathbf{r}_2)\bigg]$$
$$+\frac{1}{2}\int d^3\mathbf{r}_1 d^3\mathbf{r}_2 n(\mathbf{r}_1)n(\mathbf{r}_2)g(\mathbf{r}_1,\mathbf{r}_2)e^2G(\mathbf{r}_1|\mathbf{r}_2). \tag{106}$$

For a large plasma, the second of the three terms in this expression is much larger than the other two. It is useful to compare this term to the energy of a zero temperature mean-field plasma

$$E_R^{(0)}=e\int d^3\mathbf{r}\,\phi_R(\mathbf{r})n^{(0)}(\mathbf{r})+\frac{e^2}{2}\int d^3\mathbf{r}_1 d^3\mathbf{r}_2 n^{(0)}(\mathbf{r}_1)$$
$$\times n^{(0)}(\mathbf{r}_2)G(\mathbf{r}_1|\mathbf{r}_2), \tag{107}$$

where $n^{(0)}(\mathbf{r})$ is equal to $n_-=m\omega(\Omega_c-\omega)/2\pi e^2$ out to the surface of the cold mean-field plasma and is zero beyond. The surface is a sharp boundary because $\lambda_D=0$ for $T=0$. The cold mean-field plasma is assumed to have the same number of particles, the same rotation frequency, and the same trap parameters as the actual plasma. The density difference $\Delta n(\mathbf{r}) \equiv n(\mathbf{r}) - n^{(0)}(\mathbf{r})$ is nonzero only within a distance λ of the surface; both $n(\mathbf{r})$ and $n^{(0)}(\mathbf{r})$ must equal n_- in the plasma interior. Spatial oscillation (or simply spatial variation) of $n(\mathbf{r})$ is possible only within the surface layer, because knowledge of the surface position is necessary to define the phase of the oscillation. Thus for a large plasma, $E_R^{(0)}$ is close in value to the second term in the expression for E_R in Eq. (106).

Formally, we will show that the difference is negligible in the limit where the volume of the surface layer is negligible compared to the volume of the plasma as a whole. To this end, consider the difference

$$E_R - E_R^{(0)} = \frac{3}{2} NkT + \int d^3\mathbf{r}_1 \Delta n(\mathbf{r}_1) \Big[e\phi_R(\mathbf{r}_1) + \int d^3\mathbf{r}_2 e^2 G(\mathbf{r}_1|\mathbf{r}_2) n^{(0)}(\mathbf{r}_2) \Big] + \frac{1}{2} \int d^3\mathbf{r}_1 d^3\mathbf{r}_2 e^2 G(\mathbf{r}_1|\mathbf{r}_2) \Delta n(\mathbf{r}_1) \Delta n(\mathbf{r}_2) + \frac{1}{2} \int d^3\mathbf{r}_1 d^3\mathbf{r}_2 n(\mathbf{r}_1) n(\mathbf{r}_2) g(\mathbf{r}_1,\mathbf{r}_2) e^2 G(\mathbf{r}_1|\mathbf{r}_2). \tag{108}$$

The second term can be rewritten as $\int d^3\mathbf{r}_1 e \Delta n(\mathbf{r}_1)[\phi_R(\mathbf{r}_1) + \phi_p^{(0)}(\mathbf{r}_1)]$, where $\phi_p^{(0)}(\mathbf{r}_1)$ is the space-charge potential for the cold mean-field plasma. For a cold mean-field plasma (i.e., $\lambda_D = 0$), the condition $\nabla(\phi_R + \phi_p^{(0)}) = 0$ must hold out to the sharp bounding surface, so we set $\phi_R(\mathbf{r}) + \phi_p^{(0)}(\mathbf{r})$ equal to a constant (say, C) over the whole interior. Because the cold mean-field plasma and the actual plasma have the same number of charges, $\int d^3\mathbf{r} \Delta n(\mathbf{r})$ is zero. Thus the second term in Eq. (108) can be rewritten as

$$\int_{\text{outside}} d^3\mathbf{r}_1 e n(\mathbf{r}_1)[\phi_R(\mathbf{r}_1) + \phi_p^{(0)}(\mathbf{r}_1) - C], \tag{109}$$

where the integral is over the volume outside the cold mean-field plasma. The density $n(\mathbf{r}_1)$ is nonzero only out to a distance λ beyond the surface of the cold mean-field plasma. Near the surface, $\phi_R(\mathbf{r}) + \phi_p^{(0)}(\mathbf{r})$ differs from C only by a small amount

$$\phi_R(\mathbf{r}) \phi_p^{(0)}(\mathbf{r}) \simeq \frac{x^2}{2} (\hat{n} \cdot \nabla)^2 [\phi_R(\mathbf{r}) + \phi_p^{(0)}(\mathbf{r})], \tag{110}$$

where $\hat{n}$ is the normal to the surface and x is the distance from the surface, and the derivatives are evaluated just outside the surface. First order terms in x vanish since $\nabla(\phi_R + \phi_p^{(0)})$ is zero inside and continuous at the surface. Thus integral (109) is of order $A\lambda^3 e n_-(\hat{n}\cdot\nabla)^2[\phi_R + \phi_p^{(0)}] \sim A\lambda n_- e^2 n_- \lambda^2$, where A is the surface area of the plasma. By setting $A\lambda n_- = N\Delta V/V$, where ΔV is the volume of the correlation-length-thick surface shell and V is the volume of the plasma as a whole, and recalling that λ is of order λ_D or $\alpha n^{-1/3}$, we obtain the estimates $N(\Delta V/V)kT$ or $N\alpha^2(\Delta V/V)e^2 n^{-1/3}$. The first term in Eq. (108) is of order NkT and the last of order $Ne^2 n^{-1/3}$, so the second term is negligible for sufficiently small $\Delta V/V$.

Similarly, the third term in Eq. (108), for which the integrand is nonzero only when both $\mathbf{r}_1$ and $\mathbf{r}_2$ are within a length λ of the surface, is another surface contribution. One can see this by writing this term as

$$\frac{1}{2} \int d^3\mathbf{r}_1 d^3\mathbf{r}_2 e^2 G(\mathbf{r}_1|\mathbf{r}_2) \Delta n(\mathbf{r}_1) \Delta n(\mathbf{r}_2) = \frac{e}{2} \int d^3\mathbf{r}_2 \Delta\phi_p(\mathbf{r}_2) \Delta n(\mathbf{r}_2), \tag{111}$$

where $\Delta\phi_p(\mathbf{r}_2)$ is the potential difference caused by $\Delta n(\mathbf{r}_1)$. Writing $d^3\mathbf{r}_2$ as $d^2\mathbf{r}dx$ where $\mathbf{d}^2\mathbf{r}$ is an area element of the surface and x is a coordinate normal to the surface, we integrate by parts neglecting surface curvature, to obtain

$$-\frac{e}{2} \int d^2\mathbf{r} \int dx \frac{\partial \Delta\phi_p}{\partial x} \int_{-\infty}^{x} dx' \Delta n(x'). \tag{112}$$

Since $\partial\Delta\phi_p/\partial x \to 0$ as $x \to \pm\infty$, we replace $\partial\Delta\phi_p/\partial x$ by its maximum magnitude, $4\pi e n_-\lambda$ (this follows from the Poisson equation $\partial^2\Delta\phi/\partial x^2 \simeq -4\pi e \Delta n$). Since $\int_{-\infty}^{\infty} dx\, \Delta n(x) = 0$, we estimate $\int_{-\infty}^{\infty} dx \int_{-\infty}^{x} dx' \Delta n(x')$ to be of order $n_-\lambda^2$. Then the magnitude of the third term in Eq. (108) is of order $A\, 2\pi e^2 n_- \lambda n_- \lambda^2$, which is the same estimate that was obtained for the second term. Thus the third term also is negligible in the limit $\Delta V/V \to 0$.

Also in this limit, we can neglect contributions to the integral in the fourth term for $\mathbf{r}_1$ and $\mathbf{r}_2$ values within the surface layer. In the plasma interior, we may set $n(\mathbf{r}) = n_-$, $g(\mathbf{r}_1,\mathbf{r}_2) = g(\mathbf{r}_1 - \mathbf{r}_2)$, and $G(\mathbf{r}_1|\mathbf{r}_2) \simeq |\mathbf{r}_1 - \mathbf{r}_2|^{-1}$; so Eq. (108) reduces to the result

$$E_R - E_R^{(0)} = U_{\text{OCP}}, \tag{113}$$

where

$$U_{\text{OCP}} = \frac{3}{2} NkT + \frac{Ne^2 n_-}{2} \int d^3\mathbf{r} \frac{g(\mathbf{r})}{|\mathbf{r}|} \tag{114}$$

is the internal energy of an infinite homogeneous OCP.[11] The first term is the mean kinetic energy and the second the correlation energy. Again we note that the mean-field electrostatic energy dominates the energy of a large trapped plasma, that is, $E_R^{(0)}$ is much larger than U_{OCP}. In an OCP this mean-field energy does not appear because there really is a uniform neutralizing background charge present, and the self-energy of this background just cancels $E_R^{(0)}$.

Here we argued that the surface contribution to the free energy is small for sufficiently small $\Delta V/V$, and then we neglected this contribution. For the case of slab geometry, the surface contribution can be calculated and compared in detail to the bulk contribution. The interesting case is that of a crystal state, and for this case the plasma must be about 60 lattice planes across for the bulk free energy to dominate.[32] This is consistent with our estimate that a surface sheath for a large spheroidal plasma is a few tens of interparticle spacings.

B. Free energy of an OCP

Following custom, we denote the correlation energy by $U_{\rm corr}$ and introduce the scaled correlation energy[11,12]

$$\frac{U_{\rm corr}}{NkT}(\Gamma)=\frac{e^2 n_-}{2kT}\int d^3\mathbf{r}\,\frac{g(\mathbf{r})}{|\mathbf{r}|}, \tag{115}$$

which depends only on the coupling parameter $\Gamma=e^2/akT$. Here a is the Wigner–Seitz radius (i.e., $4\pi a^3 n/3\equiv 1$). The scaled correlation energy has been determined for the full range of Γ values and is available in the literature.[11,12]

The free-energy $F_{\rm OCP}$ is related to $U_{\rm OCP}$ through the equation [see Eq. (31)]

$$-T^2\left.\frac{\partial[F_{\rm OCP}/T]}{\partial T}\right)_{n,T}=U_{\rm OCP}(T,n,N). \tag{116}$$

By integrating with respect to T we obtain

$$\frac{F_{\rm OCP}(T,n,N)}{T}=\frac{F_{\rm OCP}(T_0,n,N)}{T}-\int_{T_0}^{T}\frac{U_{\rm OCP}}{T'^2}(T',n,N)\,dT', \tag{117}$$

where T_0 is a reference temperature where $F_{\rm OCP}$ is known. By using $dT/T=-d\Gamma/\Gamma$, we obtain

$$\frac{F_{\rm OCP}(T,n,N)}{T}=\frac{F_{\rm OCP}(T_0,n,N)}{T_0}+N\int_{\Gamma_0}^{\Gamma}\frac{U_{\rm OCP}}{NkT}(\Gamma')\,\frac{d\Gamma'}{\Gamma'}, \tag{118}$$

where the integral is now in a form that can be evaluated using the known function $U_{\rm OCP}/NkT(\Gamma)$. For a plasma in the fluid state, T_0 is chosen to be very high so that $F_{\rm OCP}(T_0,n,N)$ is the well-known free energy of a weakly correlated plasma (ideal gas).[11,12] For a plasma in a crystal state one chooses T_0 to be very low, so that $F_{\rm OCP}(T_0,n,N)$ is the well-known free energy of a harmonic lattice.[11,12]

Other thermodynamic functions are obtained in the usual manner through partial derivatives of the free energy [e.g., $S_{\rm OCP}=-\partial F_{\rm OCP}/\partial T)_{n,N}$]. For future reference, we note two of these functions here. The pressure

$$p=-\left.\frac{\partial n}{\partial V}\right)_N\left.\frac{\partial F_{\rm OCP}}{\partial n}\right)_{T,N} \tag{119}$$

is given by[12]

$$p=nkT\left[1+\frac{1}{3}\frac{U_{\rm corr}}{NkT}(\Gamma)\right]. \tag{120}$$

In the limit of weak correlation ($\Gamma\ll 1$), the second term in the bracket is negligible compared to unity, and we recover the pressure for an ideal gas, $p=nkT$. Also, we will need the specific heat at constant density[12]

$$c_n=T\left.\frac{\partial S_{\rm OCP}}{\partial T}\right)_{n,N}=Nk\left\{\frac{3}{2}-\Gamma^2\frac{\partial}{\partial\Gamma}\left[\frac{U_{\rm corr}}{NkT}(\Gamma)/\Gamma\right]\right\}, \tag{121}$$

which is easily obtained from Eqs. (114) and (115) using $T\partial S_{\rm OCP}/\partial T)_{n,N}=\partial U_{\rm OCP}/\partial T)_{n,N}$. In the limit of weak correlation, we recover the specific heat for an ideal gas $c_n=3Nk/2$.

C. Relation between the free energies

Returning to the original question of the relationship between F_R and $F_{\rm OCP}$, we note that Eqs. (31), (113), and (116) together with the fact that $E_R^{(0)}$ is independent of temperature imply the relation

$$\frac{\partial}{\partial T}\left[(F_R-F_{\rm OCP}-E_R^{(0)})/T\right]=0. \tag{122}$$

When carrying out the temperature derivative, everything else is held constant. In F_R and $E_R^{(0)}$, the quantities $(\omega,B,\{V_j\},N)$ are held constant, and in $F_{\rm OCP}$ the quantities (n,N) are held constant. One should note here that n is implicitly a function of ω and B through Eq. (12). Integrating Eq. (122) with respect to T yields the relation

$$F_R-F_{\rm OCP}-E_R^{(0)}=gT, \tag{123}$$

where g is some temperature-independent function. Using $S=-\partial F_R/\partial T$ and $S_{\rm OCP}=-\partial F_{\rm OCP}/\partial T$ then yields $S-S_{\rm OCP}=g$. Since S and $S_{\rm OCP}$ must vanish at $T=0$ according to the third law and since g is independent of T, we may conclude that $g=0$ and that

$$F_R(T,\omega,B,\{V_j\},N)=E_R^{(0)}(\omega,B,\{V_j\},N)+F_{\rm OCP}(T,n,N), \tag{124}$$

where n is an implicit function of ω and B through Eq. (12).

D. Other thermodynamic variables

The free energy is expressed in terms of the primary thermodynamic variables $\{\lambda_k\}=\{T,-\omega,B,\{V_j\},N\}$, and the conjugate variables $\{\Lambda_k\}=\{S,L,M,\{q_j\},-\mu\}$ are obtained as the partial derivatives $\Lambda_k=-\partial F_R/\partial\lambda_k$. [See Eq. (44). Note that the term ''conjugate'' is used in a slightly different sense than in Eq. (69), since there it was convenient to connect conjugate variables through derivatives of the system energy rather than the free energy. This accounts for the appearance of $-\mu$ rather than μ in the set of Λ_k.] From separation (124) we will obtain $\Lambda_k=\Lambda_k^{(0)}+\Lambda_k^{(1)}$, where

$$\Lambda_k^{(0)}=-\frac{\partial E_k^{(0)}}{\partial\lambda_k}(\omega,B,\{V_j\},N), \tag{125}$$

$$\Lambda_k^{(1)}=-\frac{\partial F_{\rm OCP}}{\partial\lambda_k}(n,T,N). \tag{126}$$

Here, all variables except λ_k are held constant when carrying out the derivatives.

Before proceeding to evaluate such derivatives, it is useful to recall the distinct properties of $E_R^{(0)}$ and $F_{\rm OCP}$. As mentioned earlier, $E_R^{(0)}$ is much larger than $F_{\rm OCP}$. Also, $E_R^{(0)}$ increases with N faster than the first power, that is, $E_R^{(0)}$ is nonextensive in the limit $N\to\infty$; whereas, $F_{\rm OCP}$ is proportional to N and so is extensive. Thus the nonextensive dependence enters only through $E_R^{(0)}$, and that dependence is particularly simple because $E_R^{(0)}$ does not depend on temperature (or on the state of correlation). $E_R^{(0)}$ is completely determined by n [or, equivalently, by $\omega(\Omega_c-\omega)$], and the shape and size of the cold mean-field plasma. The shape is determined by some combination of ω, N, B, and $\{V_j\}$. In contrast, $F_{\rm OCP}/N$ depends on n and T (and through these on the correlation state), but does not depend on plasma shape.

The entropy $S=-\partial F/\partial T)_{\omega,B,\{V_j\},N}$ is special since $E_R^{(0)}$ is independent of T. We obtain[29,8]

$$S=S^{(1)}=-\left.\frac{\partial F_{\rm OCP}}{\partial T}\right)_{n,N}=S_{\rm OCP}(T,n,N), \tag{127}$$

where use has been made of Eq. (12) to equate $\partial/\partial T)_{\omega,B}$ to $\partial/\partial T)_n$. A corollary is the result:

$$c_\omega=T\left.\frac{\partial S}{\partial T}\right)_{\omega,B,\{V_j\},N}=T\left.\frac{\partial S_{\rm OCP}}{\partial T}\right)_{n,N}=c_n, \tag{128}$$

where c_n is given in Eq. (121).

Thus $S=S_{\rm OCP}$ is extensive, and $S/N=s(n,T)$ is intensive and is determined by n and T alone regardless of the plasma shape.[8,28] In contrast, $E_R^{(0)}$ makes large (nonextensive) contributions to L, $\{q_j\}$, M, and μ. This implies large cancellations in TdS equation (45). These cancellations are embodied in the differential relation

$$O=dE_R^{(0)}-L^{(0)}d\omega+\sum_j q_j^{(0)}dV_j+M^{(0)}dB-\mu^{(0)}dN, \tag{129}$$

which follows from Eqs. (125).

After the cancellation, the Tds equation must reduce to the form

$$Tds=T\left.\frac{\partial s}{\partial T}\right)_n dT+T\left.\frac{\partial s}{\partial n}\right)_T dn. \tag{130}$$

The first coefficient can be written as

$$T\left.\frac{\partial s}{\partial T}\right)_n=\frac{T}{N}\left.\frac{\partial S_{\rm OCP}}{\partial T}\right)_{n,N}=\frac{1}{N}c_n, \tag{131}$$

where c_n is given in Eq. (121). By using Eqs. (119) and (126), the second coefficient can be written as

$$T\left.\frac{\partial s}{\partial n}\right)_T=-\frac{T}{N}\left.\frac{\partial V}{\partial n}\right)_N\left.\frac{\partial^2 F_{\rm OCP}}{\partial V\partial T}\right)_N=-\frac{T}{n^2}\left.\frac{\partial p}{\partial T}\right)_n, \tag{132}$$

where $p(n,T)$ is given in Eq. (120). Substituting into Eq. (130) yields the result

$$Tds=\frac{c_n}{N}dT+T\left.\frac{\partial p}{\partial T}\right)_n d\left(\frac{1}{n}\right), \tag{133}$$

which is well known from the thermodynamics of fluids.[33]

In Sec. IV D we evaluated the change in temperature under adiabatic changes in V_j and B. For a large plasma, the entropy per particle is only a fraction of T and n, so we should obtain the change in temperature under an adiabatic change in density;

$$0=Tds=\frac{c_n}{N}dT-\frac{T}{n^2}\left.\frac{\partial p}{\partial T}\right)_n dn. \tag{134}$$

In an uncorrelated plasma $p=nkT$ and $c_n=3/2Nk$, and we find the usual adiabatic relation between T and n for an ideal gas:

$$\left.\frac{\partial \ln T}{\partial \ln n}\right)_s=\frac{2}{3}. \tag{135}$$

However, in a strongly correlated plasma the relation is modified, since both p and c_n depend on Γ; see Eqs. (120) and (121). For $\Gamma\gtrsim 3$ the pressure actually changes sign as $U_{\rm corr}/NkT$ becomes large and negative, so one might imagine that during an adiabatic expansion the correlated plasma might actually heat rather than cool. However, this is not the case, although the rate of cooling during the expansion is reduced compared to Eq. (135).[8] In fact, using Eq. (120), Eq. (134) can be expressed succinctly in terms of the specific heat, which is nonnegative:

$$\left.\frac{\partial \ln T}{\partial \ln n}\right)_s=\left[\frac{1}{3}+\frac{1}{2}\frac{Nk}{c_n}\right]. \tag{136}$$

Adiabatic expansion has been proposed as a method of cooling trapped pure electron plasmas.

To evaluate $L^{(0)}$, $M^{(0)}$, $\{q_j^{(0)}\}$, and $\mu^{(0)}$, we need an expression for $E_R^{(0)}(\omega,B,\{V_j\},N)$, which depends on the plasma shape. Fortunately, $E_R^{(0)}$ can be calculated analytically for two geometries that are commonly used in experiment.

The first is the case of a long column. Suppose that the length of the central cylinder in Fig. 1 is much larger than the radius (i.e., $l\gg R_p$). The shape of the zero temperature mean-field plasma can then be approximated by a right circular cylinder of length l and radius R_p. The number of particles is given by

$$N=\pi R_p^2 ln, \tag{137}$$

and expression (107) for $E_R^{(0)}$ reduces to the simple form

$$E_R^{(0)}=\frac{3}{4}\frac{(Ne)^2}{l}+\frac{(Ne)^2}{l}\ln\frac{R_w}{R_p}, \tag{138}$$

where R_p is related to (N,ω,B) through Eqs. (12) and (137) and R_w is the radius of the cylindrical trap electrodes. A superscript zero has not been added to N, since by definition the cold mean-field plasma has the same number of particles as the actual plasma (i.e., $N=N^{(0)}$).

As an example of Eq. (125), we evaluate the derivatives

$$L^{(0)}=\left.\frac{\partial E_R^{(0)}}{\partial\omega}\right)_{B,\{V_j\},N}=-\frac{(Ne)^2}{2l}\frac{1}{R_p^2}\left.\frac{\partial R_p^2}{\partial\omega}\right)_{B,\{V_j\},N}=\frac{(Ne)^2\Omega_v}{2l\omega(\Omega_c-\omega)} \tag{139}$$

and

$$M^{(0)}=-\left.\frac{\partial E_R^{(0)}}{\partial B}\right)_{\omega,\{V_j\},N}=\frac{(Ne)^2}{2l}\frac{1}{R_p^2}\left.\frac{\partial R_p^2}{\partial B}\right)_{\omega,\{V_j\},N}=-\frac{(Ne)^2e}{2lmc(\Omega_c-\omega)}. \tag{140}$$

Alternatively, these results can be obtained by evaluating $L^{(0)}=m(\Omega_v/2)N\langle r^2\rangle^{(0)}$ and $M^{(0)}=-N(e\omega/2c)\langle r^2\rangle^{(0)}$ for a right circular cylinder. By explicitly carrying out the derivatives

$$\left.\frac{\partial L}{\partial\omega}\right)_{T,B,\{V_j\},N}\simeq\left.\frac{\partial L^{(0)}}{\partial\omega}\right)_{B,\{V_j\},N}$$

$$=-\frac{(Ne)^2}{2l}\frac{[(\Omega_c-\omega)^2+\omega^2]}{\omega^2(\Omega_c-\omega)^2}, \tag{141}$$

$$\left.\frac{\partial M}{\partial B}\right)_{T,\omega,\{V_j\},N}\simeq\left.\frac{\partial M^{(0)}}{\partial B}\right)_{\omega,\{V_j\},N}\simeq\frac{(Ne)^2}{2l[mc(\Omega_c-\omega)/e]^2}, \tag{142}$$

we can check that inequalities (76) and (78) are satisfied for this case. As discussed in Sec. IV B, these inequalities hold when any combination of the conjugate variables in Eq. (69) are held constant. Finally, one should note that the right circular cylinder approximation is too crude to capture the dependence of $E_R^{(0)}$ on $\{V_j\}$. A more sophisticated model would be required to evaluate $q_j^{(0)}$.

A second analytically tractable case is that of a spheroidal plasma in a quadratic trap potential (see Sec. III C). The zero temperature mean-field energy is given by

$$E_R^{(0)}=\frac{3}{10}Nm\omega_z^2[2\beta R_p^2+Z_p^2]+NC, \tag{143}$$

where ω_z, C, and β are defined in Eqs. (18) and (19) and R_p and Z_p are given as functions of β and N in Eqs. (20)–(25). For this case, we already have an expression for $L^{(0)}$ [see Eq. (27)]. This simple form was obtained by evaluating $L^{(0)}=m(\Omega_v/2)N\langle r^2\rangle^{(0)}$ directly, rather than evaluating the derivative $L^{(0)}=\partial E_R^{(0)}/\partial\omega$. Again, the derivative

$$\left.\frac{\partial L}{\partial\omega}\right)_{T,B,\{V_j\},N}\simeq\left.\frac{\partial L^{(0)}}{\partial\omega}\right)_{B,\{V_j\},N}$$

$$=-\frac{2NmR_p^2}{5}\left(1+\frac{\Omega_v^2}{3\omega_p^2}\left(2+\frac{d\ \ln\ \alpha(\beta)}{d\beta}\right)\right) \tag{144}$$

can be evaluated showing explicitly that inequality (76) is satisfied for this case. Recall that α is a monotonically increasing function of β according to Eq. (20).

This model does contain the dependence of $E_R^{(0)}$ on $\{V_j\}$ so we can evaluate $q_j^{(0)}=-\partial E_R^{(0)}/\partial V_j$. For the case of hyperbolic electrodes, where Eq. (17) may be used, we find that the induced charge on the ring and cap electrodes satisfies $q_{\rm ring}^{(0)}+q_{\rm cap}^{(0)}=-Ne$, as one would expect, and that

$$q_{\rm ring}^{(0)}-q_{\rm cap}^{(0)}=-Ne\,\frac{[z_0^2-(r_0^2/2)+(6/5)(R_p^2-Z_p^2)-(4/5)(2\beta+1)(\beta R_p^2-Z_p^2)d\ \ln\ \alpha/d\beta]}{z_0^2+r_0^2/2}. \tag{145}$$

Since the plasma is assumed to be far from the electrodes, one can see that the plasma shape has little effect on the induced charge, as expected. Also, the induced charge is completely independent of the plasma radius when the plasma is spherical, which also follows from symmetry arguments.

As an example of the finite temperature correction to these zero temperature mean-field quantities, we evaluate

$$L^{(1)}(T,\omega,B,\{V_j\},N)=\left.\frac{\partial F_{\rm OCP}}{\partial\omega}\right)_{T,B,\{V_j\},N}$$

$$=\left.\frac{\partial n}{\partial\omega}\right)_B\left.\frac{\partial F_{\rm OCP}}{\partial n}\right)_{T,N}. \tag{146}$$

With the aid of Eqs. (12) and (119), this reduces to

$$L^{(1)}(T,\omega,B,\{V_j\},N)=\frac{N\Omega_v}{\omega(\Omega_c-\omega)}\frac{p(n,T)}{n}, \tag{147}$$

where $p(n,T)$ is given in Eq. (120).

This result plus the relation $L=m(\Omega_v/2)\langle r^2\rangle$ yields the temperature correction to the mean square radius[34]

$$\langle r^2\rangle-\langle r^2\rangle^{(0)}=\frac{p(n,T)}{\pi e^2n^2}, \tag{148}$$

where use has been made of Eq. (12). This result is valid for large plasmas in any confinement geometry. For a weakly correlated plasma, where $p=nkT$ is positive, the pressure causes a slight increase in the mean-square radius $\Delta\langle r^2\rangle=kT/\pi e^2n=\lambda_D^2/4$. For a strongly correlated plasma, where $p\sim-ne^2/a$ is negative, the pressure (i.e., correlation) causes a slight decrease in the mean-square radius $\Delta\langle r^2\rangle\sim-1/na\sim-a^2$. Equation (148) was obtained first for the special case of a weakly correlated infinitely long column.[35,36]

Another example of a temperature correction is

$$q_j^{(1)}(T,\omega,B,\{V_j\},N)=-\left.\frac{\partial F_{\rm OCP}}{\partial n}\right)_{T,N}\left.\frac{\partial n}{\partial V_j}\right)_{T,\omega,B,\{V_{k\neq j}\},N}=0, \tag{149}$$

where Eq. (12) has been used to show that $\partial n/\partial V_j)_{\omega,B}=0$. Thus the charge q_j does not vary with T assuming that ω and B are held constant. However, if ω is replaced by its conjugate variable L, we obtain a nonzero correction

$$q_j^{(1)}(T,L,B,\{V_j\},N)=-\left.\frac{\partial F_{\rm OCP}}{\partial n}\right)_T\left.\frac{\partial n}{\partial V_j}\right)_{T,L,B,\{V_{k\neq j}\},N}$$

$$=-\frac{Np}{n}\frac{1}{n}\left.\frac{\partial n}{\partial V_j}\right)_{T,L,B,\{V_{k\neq j}\},N}, \tag{150}$$

where use has been made of Eq. (119) and $p(n,T)$ is given by Eq. (120). As a specific example, for an uncorrelated plasma in a hyperbolic trap, Eq. (17) can be used with Eqs. (20)–(27) to obtain

$$-q_{\rm ring}^{(1)}(T,L,B,\{V_j\},N) = q_{\rm cap}^{(1)}(T,L,B,\{V_j\},N) = -\frac{d\ \ln\ \alpha/d\beta}{d\ \ln\ \alpha/d\beta+2\omega_z^2/\omega_p^2+3\omega_z^2/\Omega_v^2}\frac{NkT}{V_0}, \tag{151}$$

where V_0 is the potential difference between the cap and ring electrode [see Eq. (17)]. Since $d\alpha/d\beta>0$ Eq. (151) implies that charge flows off the cap electrode and onto the ring electrode as temperature increases at constant L. Consequently, measurements of q_j might provide useful temperature information, although the effect is small: for $V_0=1$ V in a spherical plasma for which $\Omega_v \gg \omega_z$, Eq. (151) predicts that a temperature change of 1 K induces a charge Δq on the electrodes of magnitude $|\Delta q/eN|=5\times 10^{-5}$.

In the next section, we will need two results for large plasmas that follow simply from the extensive and nonextensive character of certain quantities. Since $\partial L/\partial\omega)_T$ is nonextensive (increasing faster than N) and $\partial L/\partial T)_\omega$ is extensive (increasing like N), Eq. (54) implies that the relative difference $|c_\omega-c_L|/Nk$ approaches zero for sufficiently large N. It may be instructive to evaluate the difference $|c_L-c_\omega|$ for the case of a long, weakly correlated plasma. Combining Eqs. (54), (147), and (141) yields the result

$$\frac{|c_\omega-c_L|}{Nk}=\frac{8(\Omega_c-2\omega)^2}{[(\Omega_c-\omega)^2+\omega^2]}\left(\frac{\lambda_D}{R_p}\right)^2 \ll 1. \tag{152}$$

Likewise, for a sufficiently large plasma we conclude that

$$\left|\frac{T}{\omega}\frac{\partial\omega}{\partial T}\right)_L\bigg| = \left|\frac{T}{\omega}\frac{\partial L/\partial T)_\omega}{\partial L/\partial\omega)_T}\right| \ll 1. \tag{153}$$

Again, for the case of a long, weakly correlated plasma, Eqs. (147) and (141) imply the result

$$\left|\left(\frac{T}{\omega}\frac{\partial\omega}{\partial T}\right)\right| = \frac{8(\Omega_c-\omega)^2}{[(\Omega_c-\omega)^2+\omega^2]}\left(\frac{\lambda_D}{R_p}\right)^2 \ll 1. \tag{154}$$

In Sec. IV C, we promised to verify Eqs. (95) and (96) for the case of a large plasma. In order to do so we first note that

$$\frac{\partial\langle G\rangle}{\partial T}\bigg)_{(\omega/T)} = \frac{\partial\langle G\rangle}{\partial T}\bigg)_\omega + \frac{\omega}{T}\frac{\partial\langle G\rangle}{\partial\omega}\bigg)_T \tag{155}$$

and

$$\frac{\partial\langle G\rangle}{\partial(\omega/T)}\bigg)_T = T\frac{\partial\langle G\rangle}{\partial\omega}\bigg)_T. \tag{156}$$

Next, we employ Jacobian transformations to write

$$\frac{\partial T}{\partial L}\bigg)_E = \frac{\partial(T,E)}{\partial(L,E)} = \frac{\partial(T,\omega)}{\partial(L,E)}\frac{\partial(T,E)}{\partial(T,\omega)} = -\frac{\partial E/\partial\omega)_T}{c_L\partial L/\partial\omega)_T} = \frac{T\partial L/\partial T)_\omega+\omega\partial L/\partial\omega)_T}{c_L\partial L/\partial\omega)_T}, \tag{157}$$

where we used Eqs. (55), (58), and (61). We can also employ Eqs. (59) and (60) to write

$$\frac{\partial\omega}{\partial L}\bigg)_E = \frac{c_\omega-\omega L/\partial T)_\omega}{c_L\partial L/\partial\omega)_T}. \tag{158}$$

When Eqs. (155)–(157) are employed in Eq. (94), we obtain

$$\langle\delta G^2\rangle_{E,L}-\langle\delta G^2\rangle_{T,\omega} = -\frac{kT^2}{c_L}\left[\frac{\partial\langle G\rangle}{\partial T}\bigg)_\omega+\frac{\omega}{T}\frac{\partial\langle G\rangle}{\partial\omega}\bigg)_T\right]^2 + kT\frac{\omega-T\partial\omega/\partial T)_L}{c_L}\left\{2\frac{\partial\langle G\rangle}{\partial\omega}\bigg)_T\left[\frac{\partial\langle G\rangle}{\partial T}\bigg)_\omega+\frac{\omega}{T}\frac{\partial\langle G\rangle}{\partial\omega}\bigg)_T\right] - \frac{\omega}{T}\left[\frac{\partial\langle G\rangle}{\partial\omega}\bigg)_T\right]^2\right\} + kT\frac{c_\omega-\omega\partial L/\partial T)_L}{c_L\partial L/\partial\omega)_T}\left[\frac{\partial\langle G\rangle}{\partial\omega}\bigg)_T\right]^2, \tag{159}$$

where here G is either q_j or M. Now, for a large plasma $c_\omega=c_L$, $\partial q_j/\partial T)_\omega=0$, and $|\partial M/\partial T)_\omega| \ll |\omega/T\partial M/\partial\omega)_T|$. The first two relations were proven in Eqs. (152) and (149), and the last follows from the Maxwell relation $\partial M/\partial T)_{\omega,B,\{V_j\},N}=\partial S/\partial B)_{T,\omega,B,\{V_j\},N}$ together with the fact that S is extensive in the large plasma limit.

When these relations are employed in Eq. (159) and small terms are dropped, we find

$$\langle\delta G^2\rangle_{E,L}-\langle\delta G^2\rangle_{T,\omega} = \left[\frac{\partial\langle G\rangle}{\partial\omega}\bigg)_T\right]^2\frac{kT}{\partial L/\partial\omega)_T}. \tag{160}$$

Since $\partial L/\partial\omega)_T \leq 0$ it follows that the fluctuations in M or q_j at fixed E and L are smaller than fluctuations at fixed T and ω. Equation (160) can be further simplified using Maxwell relations. For example, using Eq. (50) we can transform $\partial M/\partial\omega)_T$ to obtain

$$\langle\delta M^2\rangle_{E,L}-\langle\delta M^2\rangle_{T,\omega} = -\frac{\partial M}{\partial\omega}\bigg)_{T,B}\frac{\partial L}{\partial B}\bigg)_{T,\omega}\frac{kT}{\partial L/\partial\omega)_{T,B}} = kT\frac{\partial M}{\partial\omega}\bigg)_{T,B}\frac{\partial\omega}{\partial B}\bigg)_{T,L}, \tag{161}$$

where throughout we hold $\{V_j\}$ and N fixed along with the specified variables. However, $\partial M/\partial\omega)_B\partial\omega/\partial B)_L = \partial M/\partial B)_L-\partial M/\partial B)_\omega$, and when this relation is used in Eq. (161) and the result is compared to Eq. (87) we find that for a large plasma

$$\langle \delta M^2 \rangle_{E,L} = kT \left.\frac{\partial M}{\partial B}\right)_{T,L,\{V_j\},N}. \tag{162}$$

An identical argument implies that in the large plasma limit

$$\langle \delta q_j^2 \rangle_{E,L} = kT \left.\frac{\partial q_j}{\partial V_j}\right)_{T,L,\{V_{i\neq j}\},B,N} \tag{163}$$

Although these results differ from Eqs. (86) and (87), because L is fixed rather than ω in the derivatives, the right-hand sides of Eqs. (162) and (163) are non-negative according to the general arguments of Sec. IV B.

VI. THERMODYNAMIC APPROACH TO TRANSPORT

As discussed in Sec. II B, a collection of point charges that interact electrostatically in an ideal trap (time-independent and cylindrically symmetrical electrode structure and trap fields) is characterized by two constants of the motion, $H=E$ and $P_\theta=L$. However, for a real plasma in a real trap, such effects as collisions with neutrals, radiation, and interaction with small (but unavoidable) field errors produce slow changes in E and L. Also, laser beams and rotating field asymmetries are often applied to produce changes in E and L. We assume that these changes are slow compared to the time for Coulomb collisions to bring the plasma to thermal equilibrium, so the plasma evolves through a sequence of thermal equilibrium states, and the slow evolution of E and L translates to a slow evolution of T and ω. Thermodynamics provides a simple framework for the description of this late time transport. Throughout this section we assume that the particle number and trap parameters are held constant (i.e., $dN=dV_j=dB=0$), so the TdS equation reduces to the simple form given in Eq. (47).

A. Direction of evolution

In some cases, thermodynamics alone can tell us the sign of the change in quantities and the direction of evolution. As a simple example, consider the sign of the torque that a static field error (asymmetry) exerts on a rotating plasma. Of course, one's intuition is that the torque is a drag that opposes the rotation, but how can we prove this? Fundamentally, the intuition is an expression of the second law of thermodynamics. Since the field asymmetry is static, that is, does not introduce explicit time dependence into H, H is still a constant of the motion and we can set $dE=\langle dH\rangle=0$ in Eq. (47) to obtain the result

$$0 \leqslant TdS = \omega dL = -(-\omega) dL, \tag{164}$$

where the inequality expresses the second law. Thus the plasma rotation frequency $(-\omega)$ and dL have opposite signs, that is, the torque $\dot{L}=dL/dt$ opposes the rotation. For a plasma of positive charges, the rotation frequency is negative (i.e., $\omega>0$) so $\dot{L}$ is positive.

Next, let us suppose that some other effect, say, laser cooling, maintains the plasma temperature at a constant value without exerting a torque. Then the relation $\dot{\omega} = (\partial\omega/\partial L)_T \dot{L}$ plus the inequalities $(\partial\omega/\partial L)_T \leqslant 0$ and $\dot{L}>0$ imply that $\dot{\omega}$ is negative. The stationary field asymmetry slows the plasma rotation much as a caliper brake slows the rotation of a freely spinning bicycle wheel.

To make this discussion more concrete, let us reexamine Fig. 5. Suppose that the torque laser is turned off when the plasma rotation frequency is at the far right of the curve, that is, ω is large. The plasma is then subject to the unbalanced torque of ambient field errors so $\dot{L}>0$. Further, suppose that the cooling laser, which exerts negligible torque, is left on and maintains the temperature at some low fixed value. Our analysis then predicts that the plasma frequency decreases monotonically, and such evolution is observed.

For fixed T, the direction of evolution of ω determines the direction of evolution of all other quantities. For example, from Fig. 5, one can see that starting at large ω, $R_p(t)$ decreases until $\omega(t)=\Omega_c/2$ and then $R_p(t)$ increases. Incidentally, this kind of radial evolution is not limited to the case of a quadratic trap potential. Inequality (90) together with $\dot{\omega}<0$ implies that

$$\frac{d\langle r^2\rangle}{dt} = \left.\frac{\partial \langle r^2\rangle}{\partial \omega}\right)_T \frac{d\omega}{dt} \tag{165}$$

is negative for $\omega(t)>\Omega_c/2$ and positive for $\omega(t)<\Omega_c/2$.

The use of a rotating field asymmetry, say, $\phi_0(r,z,\theta+\omega_0 t)$, has proven to be an effective way of exerting a torque that counteracts the torque due to static field asymmetries.[3,4] When the rotating field asymmetry is applied (but there are no static asymmetries), the new trap potential is $\phi_T(r,\theta,z,t)=\phi_T(r,z)+\phi_0(r,z,\theta+\omega_0 t)$. The Hamiltonian is then time dependent so $E=\langle H\rangle$ is not constant. However, the Hamiltonian in a frame that rotates with frequency $-\omega_0$ [i.e., $H'=H+\omega_0 P_\theta$] is time independent so $E'=E+\omega_0 L$ is constant. Substituting $0=dE'=dE+\omega_0 dL$ into Eq. (47) and again imposing the second law yields the result

$$0 \leqslant TdS = -(\omega_0-\omega) dL. \tag{166}$$

Thus the torque opposes the differential rotation. For example, the torque is in the same direction as the plasma rotation if the field asymmetry rotates faster than the plasma. Not surprisingly, when a cooling mechanism maintains T at a fixed value without exerting an additional torque, the inequality $\partial L/\partial\omega)_T \leqslant 0$ implies that the plasma rotation frequency evolves monotonically to the rotation frequency of the asymmetry, ω_0.

It is important to remember that the rotating asymmetry does work whenever it exerts a torque [i.e., $\dot{E}=\omega_0 \dot{L}_0$]. If the rotating asymmetry is used to counteract ambient torques, say, due to static field errors, then the plasma can remain in steady state only if a cooling mechanism extracts energy at the rate $\omega_0 \dot{L}_0$.

Equation (166) also can be derived by using the thermodynamic potential Ω_R, that was defined in Eq. (68). One treats the field asymmetry and the process that maintains the temperature at a fixed value as a heat and angular momentum reservoir. The reservoir is assumed to be fixed at the initial temperature T of the plasma and the rotation frequency $-\omega_0$ of the field error. The heat transfer is assumed to be sufficiently effective that the plasma remains in temperature equilibrium with the reservoir even though it is not in frequency equilibrium with the reservoir. The thermodynamic potential Ω_R must decrease as the plasma evolves toward frequency equilibrium with the reservoir. Thus we obtain

$$0 \geqslant \Delta\Omega_R = \left.\frac{\partial \Omega_R}{\partial L}\right)_{T,N,B,\{V_j\}} \Delta L = -(\omega-\omega_0)\Delta L, \tag{167}$$

where the partial derivative was evaluated by setting $\lambda_k = L$, $T=T_0$, $V_j = V_{j0}$, and $B=B_0$ in Eq. (72). Again, we find that the torque opposes the differential rotation, which together with the inequality $\partial\omega/\partial L)_T \leqslant 0$ implies that the rotation frequency of the plasma evolves toward that of the field asymmetry.

B. Evolution equations

If the plasma passes through a sequence of thermal equilibrium states characterized by fixed values of N, $\{V_j\}$, and B, the temperature and rotation frequency at any instant can be expressed as $T=T(E,L)$ and $\omega=\omega(E,L)$. The time derivative of these equations,

$$\dot{T} = \left.\frac{\partial T}{\partial E}\right)_L \dot{E}(\omega,T,\chi_j) + \left.\frac{\partial T}{\partial L}\right)_E \dot{L}(\omega,T,\chi_j), \tag{168}$$

$$\dot{\omega} = \left.\frac{\partial \omega}{\partial E}\right)_L \dot{E}(\omega,T,\chi_j) + \left.\frac{\partial \omega}{\partial L}\right)_E \dot{L}(\omega,T,\chi_j), \tag{169}$$

governs the plasma evolution, where $\dot{E}=\dot{E}(\omega,T,\chi_j)$ and $\dot{L}=\dot{L}(\omega,T,\chi_j)$ are functions that describe the rate of energy and angular momentum exchange with various external agencies. For example, suppose that the plasma energy and angular momentum are changing as a result of collisions with neutrals. $\dot{E}$ and $\dot{L}$ then depend on the plasma state (i.e., on ω and T) and on some parameters χ_j that characterize the neutrals, such as the neutral density and temperature. Likewise, for interaction with a laser beam, $\dot{E}$ and $\dot{L}$ are determined by the plasma state (i.e., ω and T) and by parameters χ_j such as the intensity and frequency of the laser light. Assuming that the parameters χ_j are constant, or known functions of time, the plasma evolution is governed by two ordinary differential equations for the time evolution of T and ω. This reduction in complexity from the partial differential equations typically required to describe transport is possible because the plasma passes through a sequence of thermal equilibrium states.

With the aid of Eqs. (55)–(60), (157) and (158), Eqs. (168) and (169) can be rewritten as

$$c_L\dot{\omega} = \left[c_\omega \left.\frac{\partial \omega}{\partial L}\right)_T + \omega \left.\frac{\partial \omega}{\partial T}\right)_L \right] \dot{L} + \left.\frac{\partial \omega}{\partial T}\right)_L \dot{E}, \tag{170}$$

$$c_L\dot{T} = A\omega\dot{L} + \dot{E}, \tag{171}$$

where

$$A = 1 - \frac{T}{\omega}\left.\frac{\partial \omega}{\partial T}\right)_L . \tag{172}$$

It is often more convenient to write Eq. (170) as

$$\dot{\omega}\left(\frac{\partial L}{\partial \omega}\right)_T = \dot{L} - \left(\frac{\partial L}{\partial T}\right)_\omega \dot{T}, \tag{173}$$

where use has been made of Eqs. (54) and (171). This equation could have been written down directly by taking the time derivative of the mixed function $\omega=\omega(L,T)$. By using Maxwell relations, the coefficients of Eqs. (171) and (173) can be written in many ways. However, one can see that only c_ω and the function $L=L(\omega,T)$ are needed to evaluate the coefficients.

For the case of a large plasma, Eqs. (128), (152), (153), and (147) imply that evolution equations (171) and (173) reduce to the simple form

$$c_n\dot{T} = \dot{E} + \omega\dot{L}, \tag{174}$$

$$\dot{\omega}\left.\frac{\partial L}{\partial \omega}\right)_T = \dot{L} - \frac{N(\Omega_c-2\omega)}{\omega(\Omega_c-\omega)}\frac{1}{n}\frac{\partial p}{\partial T}\dot{T}, \tag{175}$$

where $p(n,T)$ and $c_n(n,T,N)$ are given in Eqs. (120) and (121). Here, the n dependence in p and c_n is determined by ω through Eq. (12). For the special case of a weakly correlated plasma, c_n and $(1/n)(\partial p/\partial T)$ are the constants $3Nk/2$ and k, respectively. In Eqs. (174) and (175) only the coefficient $\partial L/\partial\omega)_T \simeq \partial L^{(0)}/\partial\omega$ depends on the plasma shape; the other coefficients are explicit functions of ω and T that are independent of plasma shape. Also, we have explicit expressions for $\partial L^{(0)}/\partial\omega$ for the case of a long plasma [see Eq. (141)] and for the case of a spheroidal plasma [see Eq. (144)].

As an application of these equations, let us return to the example considered in the last section. A static field error acts on the plasma producing a positive torque ($\dot{L}>0$), and a cooling laser maintains the temperature at some fixed value without exerting a torque. From Eq. (174), one can see that energy extraction, rather than input, is required. Setting $\dot{T}=0$ immediately yields $\dot{E}=-\omega\dot{L}<0$. As discussed earlier, a static field error cannot change E, so the cooling laser alone produces $\dot{E}$. Note that energy must be extracted whether $\langle r^2\rangle$ is decreasing (for $\omega>\Omega_c/2$) or increasing (for $\omega<\Omega_c/2$). When $\langle r^2\rangle$ is decreasing, the electrostatic energy is increasing, but the rotational kinetic energy is decreasing fast enough that the total energy is decreasing.

Next suppose that the cooling laser is turned off. For $\dot{E}=0$, Eqs. (174) and (175) reduce to the form

$$\dot{T} = \frac{\omega\dot{L}}{c_n} > 0. \tag{176}$$

$$\frac{\dot{\omega}}{\omega} = \frac{T[c_n - [N(\Omega_c-2\omega)/(\Omega_c-\omega)](1/n)\partial p/\partial T]}{\omega^2\partial L/\partial\omega)_T}\frac{\dot{T}}{T}, \tag{177}$$

where $\omega\dot{L}>0$ and $c_n>0$ have been used. For a large plasma, the coefficient of $\dot{T}/T$ on the right-hand side of Eq. (177) is small. The numerator is extensive (increasing like N) and the denominator is nonextensive (increasing faster than N) so the ratio becomes small for large N. A simple estimate for the case of a weakly correlated plasma [along the lines of the estimates in Eqs. (152) and (154)], shows that the coefficient is smaller than $O(\lambda_D/R_p)^2 \ll 1$. Thus Eq. (177) implies that $|\dot{\omega}/\omega| \ll |\dot{T}/T|$; the plasma temperature rises substantially before the rotation frequency can change by a significant amount.

Nevertheless, it is interesting to consider the sign of $\dot{\omega}$. Eliminating $\dot{T}$ yields the relation

$$\dot{\omega} = \frac{c_n - [N(\Omega_c - 2\omega)/(\Omega_c - \omega)](1/n)\partial p/\partial T}{c_n(\partial L/\partial\omega)_T} \dot{L}. \quad (178)$$

The coefficient of $\dot{L}$ is simply $\partial\omega/\partial L)_E$, as can be seen by taking the time derivative of $\omega = \omega[L, T(L,E)]$ holding E constant. Thermodynamic inequalities (81) and (83) insure that $\partial\omega/\partial L)_T \leq 0$ and that $\partial(\omega/T)/\partial L)_E \leq 0$, but $\partial\omega/\partial L)_E$ can be either positive or negative.

For simplicity we evaluate the coefficient in the limit of weak correlation. For $c_n = 3Nk/2$ and $p = nkT$ the coefficient reduces to

$$\left.\frac{\partial\omega}{\partial L}\right)_E = \frac{\Omega_c + \omega}{3(\Omega_c - \omega)(\partial L/\partial\omega)_T} < 0. \quad (179)$$

Since $\dot{L}$ is positive, $\dot{\omega}$ is negative. The static field error reduces the rotation frequency as it did when the cooling laser was on. However, suppose that the plasma has cooled to the point where all of the charges are in the lowest Landau level (i.e., $kT \ll \hbar\Omega_c$). In this case, a quantum mechanical expression for F_{OCP} must be used and the expression for c_n is modified. Only one degree of freedom per particle participates in the thermal motion, so the specific heat is $c_n = Nk/2$. The pressure is still given by $p = nkT$. Substituting into Eq. (179) yields the coefficient

$$\left.\frac{\partial\omega}{\partial L}\right)_E = -\frac{(\Omega_c - 3\omega)}{(\Omega_c - \omega)(\partial L/\partial\omega)_T}, \quad (180)$$

which is positive for $\omega < \Omega_c/3$. Surprisingly, the torque due to the static field error increases the rotation frequency. Of course, the accompanying heating rapidly raises the particles out of the lowest Landau level, and then the rotation frequency begins to decrease.

C. Temperature and frequency stability

Often there is a competition between various effects. For example, radiation pressure from a laser exerts a torque that compensates the torque from collisions with neutrals or interaction with field errors. Also, cyclotron radiation or laser cooling may balance various heating effects. We search for stable stationary states, that is, states for which $\dot{T} = \dot{\omega} = 0$ and for which small deviations from equilibrium, $\delta\omega$ and δT, are damped. As we will see, the issue of stability is important. Instabilities are observed when a parameter χ_j characterizing an applied torque or cooling process is slowly varied and the equilibrium location evolves in (ω, T) space. When the location enters an unstable region, either ω or T (or both) can vary rapidly (''jump'') across the region to the next stable equilibrium.

Suppose that $\dot{E}(\omega,T)$ and $\dot{L}(\omega,T)$ are known functions and that (ω', T') is an equilibrium point where $\dot{E} = \dot{L} = 0$ and, therefore, where $\dot{T} = \dot{\omega} = 0$. To investigate stability near this point, we set $\delta\omega = \omega - \omega'$ and $\delta T = T - T'$, linearize Eqs. (174) and (175) with respect to $\delta\omega$ and δT, and assume that these quantities vary in time as $e^{\nu t}$. The result is

$$\left[c_n \nu - \left.\frac{\partial \dot{E}}{\partial T}\right)_\omega - \omega \left.\frac{\partial \dot{L}}{\partial T}\right)_\omega \right] \delta T = \left[\omega \left.\frac{\partial \dot{L}}{\partial \omega}\right)_T + \left.\frac{\partial \dot{E}}{\partial \omega}\right)_T \right] \delta\omega, \quad (181)$$

$$\left[\left.\frac{\partial L}{\partial \omega}\right)_T \nu - \left.\frac{\partial \dot{L}}{\partial \omega}\right)_T \right] \delta\omega = \left[\left.\frac{\partial \dot{L}}{\partial T}\right)_\omega - \alpha\nu \right] \delta T, \quad (182)$$

where

$$\alpha = \frac{N(\Omega_c - 2\omega)}{\omega(\Omega_c - \omega)} \frac{1}{n} \frac{\partial p}{\partial T}. \quad (183)$$

Setting the determinant of the coefficients equal to zero yields a quadratic equation for ν:

$$a\nu^2 + b\nu + c = 0, \quad (184)$$

where

$$a = c_n \left.\frac{\partial L}{\partial \omega}\right)_T, \quad (185)$$

$$b = \left\{ -\left.\frac{\partial \dot{L}}{\partial \omega}\right)_T c_n - \left.\frac{\partial L}{\partial \omega}\right)_T \left[\omega \left.\frac{\partial \dot{L}}{\partial T}\right)_\omega + \left.\frac{\partial \dot{E}}{\partial T}\right)_\omega \right] + \alpha \left[\omega \left.\frac{\partial \dot{L}}{\partial \omega}\right)_T + \left.\frac{\partial \dot{E}}{\partial \omega}\right)_T \right] \right\}, \quad (186)$$

$$c = \left.\frac{\partial \dot{L}}{\partial \omega}\right)_T \left.\frac{\partial \dot{E}}{\partial T}\right)_\omega - \left.\frac{\partial \dot{L}}{\partial T}\right)_\omega \left.\frac{\partial \dot{E}}{\partial \omega}\right)_T. \quad (187)$$

The two solutions to Eq. (184) are

$$\nu = \frac{-b \pm \sqrt{b^2 - 4ac}}{2a}, \quad (188)$$

and stability requires $\mathrm{Re}(\nu) \leq 0$ for both solutions. Inequalities (75) and (81) imply that $a \leq 0$, so stability requires $b < 0$ and $c < 0$.

As a simple example, consider the case where the angular momentum may be considered constant on the time scale required for significant changes in the energy. Setting $\dot{L} = 0$ in Eqs. (186) and (187) yields $c = 0$ and

$$b = -\left.\frac{\partial L}{\partial \omega}\right)_T \left.\frac{\partial \dot{E}}{\partial T}\right)_\omega + \left.\frac{\partial L}{\partial T}\right)_\omega \left.\frac{\partial \dot{E}}{\partial \omega}\right)_T = -\left.\frac{\partial L}{\partial \omega}\right)_T \left.\frac{\partial \dot{E}}{\partial T}\right)_L. \quad (189)$$

The nonzero root is $\nu = -b/a$, which is stable for $b < 0$, or $\partial\dot{E}/\partial T)_L < 0$ since $\partial L/\partial\omega)_T < 0$. Temperature fluctuations about the equilibrium are damped for $\partial\dot{E}/\partial T)_L < 0$, since a positive δT leads to a negative $\delta\dot{E} = \partial\dot{E}/\partial T)_L \delta T$, which restores the equilibrium. From Eq. (173) one can see that the fluctuations δT and $\delta\omega$ are coupled and vary in such a way that $0 = \delta L = \partial L/\partial\omega)_T \delta\omega + \partial L/\partial T)_\omega \delta T$.

Of course, for this case of constant L, it is simpler to replace evolution equations (174) and (175) with $c_n \dot{T} = \dot{E}(T,L)$ and $L(\omega,T) = \mathrm{constant}$. This separates out the temperature evolution at the outset and the stability results

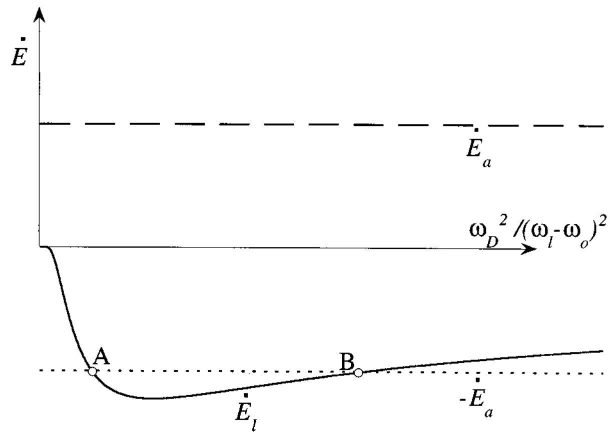

FIG. 7. A construction used to determine temperature equilibria and stability. The solid curve is a plot of the laser cooling rate $\dot{E}_l(T,L)$ versus $\omega_D^2/(\omega_l-\omega_0)^2 \propto T$, assuming that the angular momentum L is constant on the time scale of interest. The dashed curve is an ambient heating rate, $\dot{E}_a(T,L)$, assumed constant for simplicity, and the dotted curve is $-\dot{E}_a$. Points A and B are equilibria since $\dot{E}_l+\dot{E}_a=0$ at these points. Equilibrium A is stable since $\partial\dot{E}_l/\partial T)_L+\partial\dot{E}_a/\partial T)_L<0$; whereas, B is unstable since $\partial\dot{E}_l/\partial T)_L+\partial\dot{E}/\partial T)_L>0$.

follow trivially from the Taylor expansions: $c_n\delta\dot{T}=\partial\dot{E}/\partial T)_L\delta T$ and $0=\partial L/\partial\omega)_T\delta\omega+\partial L/\partial T)\delta T$.

As an illustration, we suppose that a plasma of partially ionized atoms is heated by some ambient process at the rate $\dot{E}_a(T,L)$ and laser cooled at the rate[37]

$$\dot{E}_l=\frac{NI\sigma_0}{\hbar\omega_l}\int_{-\infty}^{+\infty}\frac{dv_z(\hbar k_l v_z+2R)\exp[-v_z^2/u^2]}{[1+(\omega_l-\omega_0'-k_l v_z)^2(4/\gamma_0^2)]\sqrt{\pi}u}, \tag{190}$$

where I, ω_l, and $k_l=\omega_l/c$ are the intensity, frequency, and wave number of the laser light. The laser light is assumed to be directed along the trap magnetic field and the intensity to be uniform over the cross section of the plasma. In this case, the laser light does not exert a torque on the plasma, and the cooling rate does not depend on the plasma rotation frequency. The laser frequency is tuned near to but slightly lower than an electric dipole transition of the partially ionized atoms that constitute the plasma. The transition is characterized by the cross section at resonance σ_0, the frequency $\omega_0/2\pi$, and the line width γ_0. We define $\omega_0'=\omega_0+R/\hbar$ where $R=(\hbar k_l)^2/2m_i$. The distribution of ion-velocities parallel to $\mathbf{B}$ is Maxwellian with thermal spread $u=\sqrt{2T/m_i}$.

We define the thermal Doppler width $\omega_D=k_l u$, and for simplicity work in the limit where γ_0, $R/\hbar\ll\omega_D$. Equation (190) then reduces to the form

$$\dot{E}_l=\frac{NI\sigma_0}{\hbar\omega_l}\frac{\sqrt{\pi}\gamma_0}{2}\frac{\hbar(\omega_l-\omega_0)}{\omega_D}e^{-(\omega_l-\omega_0)^2/\omega_D^2}. \tag{191}$$

From this form one can see that $\dot{E}_l$ can be negative and substantial only if $\omega_l-\omega_0$ is negative but $|\omega_l-\omega_0|$ is not too large compared to ω_D.

In Fig. 7, the solid curve is a plot of $\dot{E}_l$ versus $\omega_D^2/(\omega_l-\omega_0)^2\propto T$. The dashed and dotted curves are plots of $\dot{E}_a(T,L)$ and $-\dot{E}_a(T,L)$, respectively, assumed here to be constant for simplicity. The intersections A and B are equilibrium points where $\dot{E}_l+\dot{E}_a=0$. Point A is stable since $\partial\dot{E}_l/\partial T)_L+\partial\dot{E}_a/\partial T)_L<0$ and point B is unstable since $\partial\dot{E}_l/\partial T)_L+\partial\dot{E}_0/\partial T)_L>0$. From the evolution equation $c_n\dot{T}=\dot{E}_l+\dot{E}_a$, one can see that the temperature will evolve to point A if it is started off at any point to the left of B. When started off at any point to the right of B, the temperature increases indefinitely.

In experiments,[37] the temperature for a plasma in stable equilibrium A is gradually reduced by slowly decreasing $|\omega_l-\omega_0|$. One can see from Eq. (191) that ω_D tracks $|\omega_l-\omega_0|$. If the slow decrease in $|\omega_l-\omega_0|$ is made through increments, one must be careful not to leave the temperature to the right of point B after the increment, that is, the increments should be smaller than $O(\omega_D)$. This can be restrictive for small ω_D. Of course, for sufficiently small ω_D, expression (191) does not accurately represent integral (190).

As another example where the stability criterion is easy to understand physically, consider the case where there is a strongly stable mechanism for temperature control, that is, $(\partial\dot{E}/\partial T)_\omega$ is negative and substantially larger in magnitude than the other terms to which it is compared in Eqs. (186) and (187). The solution for the plus sign,

$$\nu_+=\left.\frac{\partial\dot{E}}{\partial T}\right)_\omega \Big/ c_{\dot{n}}, \tag{192}$$

$$\left.\frac{\partial L}{\partial\omega}\right)_T\delta\omega+\left.\frac{\partial L}{\partial T}\right)_\omega\delta T=0, \tag{193}$$

describes strongly damped temperature and frequency fluctuations that conserve the angular momentum. In effect, this is the solution that we considered in the previous example. The solution for the minus sign,

$$\nu_-=\frac{\partial\dot{L}/\partial\omega)_T}{\partial L/\partial\omega)_T}, \tag{194}$$

$$\delta T\simeq 0, \quad \delta\omega\neq 0, \tag{195}$$

describes weakly damped or growing $(|\nu_-|\ll|\nu_+|)$ frequency fluctuations that are decoupled from the temperature fluctuations. Since $\partial L/\partial\omega)_T<0$ stability requires that $\partial\dot{L}/\partial\omega)_T>0$. This result is well known from the analysis of induction electric motors as the condition for frequency stability; recall, here, that $-\omega$ is the frequency of rotation.

Again, the analysis can be simplified at the outset by noting that the temperature is effectively fixed. The time derivative of $L(\omega,T)$, holding T fixed, yields the evolution equation $\dot{\omega}\partial L/\partial\omega)_T=\dot{L}(\omega,T)$, and Taylor expansion about the equilibrium yields solution (194).

As a specific illustration, we suppose that two laser beams act on the plasma. The first is an intense cooling beam that is directed along $\mathbf{B}$ and provides strongly stable temperature control, that is, provides a large and negative $\partial\dot{E}/\partial T)_\omega$. This beam effectively fixes T at some low value, but does not exert a torque. The second is a narrow beam that is directed transverse to $\mathbf{B}$ and passes through the plasma at a distance d from the axis. The direction of propagation is in the same sense as the plasma rotation; so the torque due to

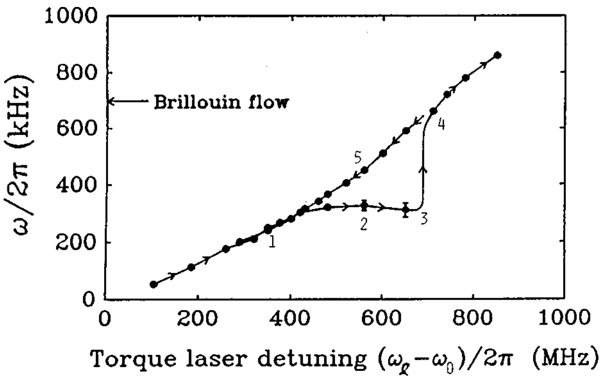

FIG. 8. Observed plasma rotation frequency versus frequency of torque laser. First the laser frequency was gradually increased then gradually decreased, and the arrows indicate the direction of evolution when the plasma rotation frequency was measured. The interesting feature is the hysteresis loop. This result is from Heinzen *et al.* (Ref. 2).

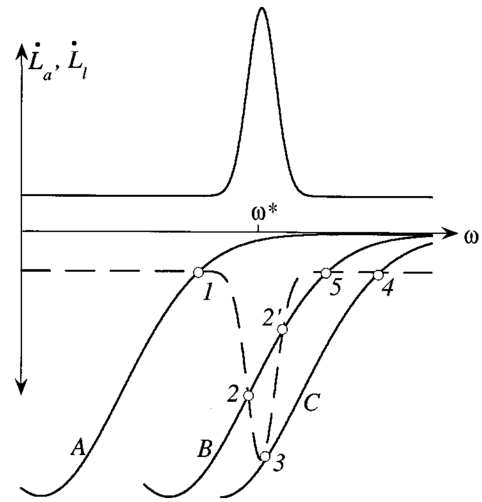

FIG. 9. A construction used to determine frequency equilibria and stability when the temperature is fixed. The solid curve in the upper half of the figure is a plot of an ambient torque $\dot{L}_a(\omega)$ assumed to have a resonance peak, and the dashed curve in the lower half is its negative $-\dot{L}_a(\omega)$. The three solid curves in the lower half of the figure are plots of a laser torque $\dot{L}_l(\omega,\omega_l)$ for three values of ω_l (i.e., $\omega_{lA}<\omega_{lB}<\omega_{lC}$). Each intersection of the dashed curve with a solid curve is an equilibrium, where $\dot{L}_l(\omega,\omega_l)+\dot{L}_a(\omega)=0$. Equilibria 1, 2, 3, 4, and 5 are stable since $\partial\dot{L}_l/\partial\omega+\partial\dot{L}_a/\partial\omega>0$; whereas, $2'$ is unstable since $\partial\dot{L}_l/\partial\omega+\partial\dot{L}_a/\partial\omega<0$. The equilibria are realized sequentially when ω_l is first increased and then decreased, and this gives rise to the hysteresis loop in Fig. 8.

the radiation pressure can balance an ambient torque, say, due to a static field error. Of course, the ambient torque opposes the rotation. The second beam can heat or cool the plasma depending on how frequencies are adjusted.

For the simple case where γ_0, $R/\hbar \ll \omega_D$, the torque is given by[38]

$$\dot{L}_l \simeq \frac{-I\sigma_0\sqrt{\pi}\gamma_0}{\hbar\omega_l 2\omega_D}\,\overline{n}_x(T,\omega,d)a\hbar k_l d e^{-(\omega_l-\omega_0-k_l d\omega)^2/\omega_D^2}, \tag{196}$$

where a is the cross-sectional area of the narrow laser beam, and

$$\overline{n}_x(T,\omega,d)=\int d^3\mathbf{r}\,\delta(y-d)\,\delta(z)\,n(\mathbf{r},\omega,T) \tag{197}$$

is the line integral of the plasma density along the beam. In writing Eq. (196), we used the fact that the x component of the plasma rotation velocity is given by $\hat{x}\cdot\omega r_\perp\hat{\theta}=\omega r_\perp\cos\theta=\omega d$ all along the beam.

In essence, this is the kind of laser system that was used to generate the experimental points in Fig. 5, where the plasma rotation frequency was varied through the full range of allowed values.[2] A slight complication is that there were two cooling beams and neither was directed parallel to B. However, both beams passed through the center of the plasma and provided strong cooling, as given by Eq. (190), with very small torque. The dominant torque was provided by an off-axis transverse beam of the kind assumed in Eq. (196). Further results from this experiment can be understood from the criterion for frequency stability. Figure 8 shows a plot of the plasma rotation frequency versus the frequency of the torque laser. Interestingly, the function $\omega=\omega(\omega_l)$ exhibits hysteresis behavior, with different values of ω obtained for the same value of ω_l depending on whether ω_l is slowly increasing or slowly decreasing. It is this behavior that we will try to understand.

The condition for frequency equilibrium is that the laser torque just balance the ambient torque

$$\dot{L}_l(\omega,\omega_i)+\dot{L}_a(\omega)=0, \tag{198}$$

and the condition for frequency stability is that

$$\frac{\partial\dot{L}_l}{\partial\omega}+\frac{\partial\dot{L}_a}{\partial\omega}>0. \tag{199}$$

Dependence on T (or ω_D) is not denoted since we assume that the intense cooling laser effectively fixes the value of T.

The experiments[2] suggest that the ambient torque is due to a field error (tilt in the magnetic field relative to the axis of the cylindrical electrode structure) and that the ambient torque becomes large (exhibits a resonance) near a particular value of the plasma rotation frequency ($\omega=\omega^*$). At this frequency, a tilt mode, which rotates backwards on the rotating plasma, has zero frequency in the laboratory frame and is driven secularly by the static field error. The amplitude of this mode presumably is limited by viscous effects, which also set the frequency width of the resonance. The solid curve in the upper half of Fig. 9 is a sketch of an ambient torque $\dot{L}_a(\omega)$ with a resonance peak at $\omega=\omega^*$, and the dashed curve in the lower half is $-\dot{L}_a(\omega)$, which is introduced for construction purposes. The three solid curves in the lower half of the figure are plots of $\dot{L}_l(\omega,\omega_l)$ as given by Eq. (196) for three values of ω_l (i.e., $\omega_{lA}<\omega_{lB}<\omega_{lC}$). To avoid confusion, the full Maxwellian is drawn only for curve A.

Each intersection of a solid curve with the dashed curve is an equilibrium point, that is, a solution of Eq. (198). For curve A, one can see graphically that equilibrium 1 is stable, that is, that $\partial\dot{L}_l/\partial\omega+\partial\dot{L}_a/\partial\omega>0$. Recall, here, that the dashed curve is $-\dot{L}_a(\omega)$. This equilibrium is indicated by point 1 in Fig. 8. When the laser frequency is increased to

ω_{lB}, equilibrium 1 evolves to equilibrium 2, which also is stable. Here the equilibrium point is climbing the resonance peak, so an increase in ω_l produces relatively little change in ω; see point 2 in Fig. 8. Curve B has two other equilibria; one can see graphically that $2'$ is unstable and 5 is stable. When the laser frequency is increased to ω_{lC}, the equilibrium evolves to point 3, which is on the edge of the stability boundary. A slight increase in ω_l produces instability, and the equilibrium jumps to equilibrium 4, the next stable equilibrium. This jump produces the nearly vertical section ($3 \rightarrow 4$) of the curve in Fig. 8. For further increase in ω_l, ω simply tracks ω_l as before the resonance. When the process is reversed by decreasing ω_l, only a small jump is encountered. Note that for decreasing ω_l, equilibrium 4 evolves into equilibrium 5, which is stable. For a sufficiently narrow resonance the small jump encountered for decreasing ω_l would not be apparent in Fig. 8.

VII. ADDITIONAL CONSTANTS OF THE MOTION

For particular confinement configurations, the plasma dynamics is characterized by additional constants (or near constants) of the motion. In a thermodynamic description, these quantities become new thermodynamic variables, just as the original constants (E and L) become thermodynamic variables.

A. Center-of-mass motion for plasma confined in a quadratic trap potential

As a first example, we consider a plasma that resides in a quadratic trap potential [see Eq. (16)] and is small compared to the distance to the electrodes. We allow the center of mass of the plasma, $\mathbf{R}_{\rm cm}=(R,\Theta,Z)$, to be displaced from the bottom of the potential well but assume that the displacement is small compared to the distance to the electrodes. Image forces are then small (we assume negligible), and the center-of-mass motion decouples from the other degrees of freedom.[39] The total plasma energy and angular momentum of a single species plasma can be written as

$$E_{\rm total}=E_{\rm cm}+E, \tag{200}$$

$$L_{\rm total}=L_{\rm cm}+L, \tag{201}$$

where

$$E_{\rm cm}=\frac{Nm}{2}\,(\dot{Z}^2+R^2\dot{\Theta}^2+\dot{R}^2)+\frac{Nm}{2}\,\omega_z^2\left(Z^2-\frac{R^2}{2}\right) \tag{202}$$

and

$$L_{\rm cm}=NmR^2\dot{\Theta}+\frac{NeBR^2}{2c} \tag{203}$$

are the center-of-mass energy and angular momentum and E and L are the energy and angular momentum relative to the center of mass. In other words, E and L are obtained from Eqs. (2)–(5) by replacing the usual cylindrical coordinates by cylindrical coordinates with an origin at the plasma center of mass and with a z axis parallel to the trap axis, without changing the functional forms of H, P_θ, A_θ, or $\phi_{\rm trap}$. Except for the use of coordinates and velocities relative to the center of mass, E and L are the same as the quantities that were called E and L in the previous sections. Since the center-of-mass motion decouples from the other degrees of freedom, $E_{\rm total}$, $L_{\rm total}$, $E_{\rm cm}$, and $L_{\rm cm}$ are all conserved independently.

Furthermore, the center-of-mass motion parallel to the magnetic field decouples from the other two degrees of freedom for the center of mass, so there is another constant of the motion.[39,17] By using the Hamilton–Jacobi equation,[18] one can show that

$$E_{\rm cm}=\omega_z I_z-\omega_m L_{\rm cm}+\omega_r I_r, \tag{204}$$

where $(I_z,L_{\rm cm},I_r)$ are the three conserved actions associated with the parallel motion, azimuthal (or magnetron) motion, and radial motion of the center of mass. Here ω_z is the frequency of the parallel motion of the center of mass, and $\omega_r=\sqrt{\Omega_c^2-2\omega_z^2}$ is the frequency of the radial motion. The quantity $\omega_m=\Omega_c/2-\sqrt{(\Omega_c/2)^2-\omega_z^2/2}$ is the magnetron frequency, but, as is our custom for rotation frequencies, a minus sign has been introduced so that $-\omega_m=\partial E_{\rm cm}/\partial L_{\rm cm}$ is the rotation frequency associated with the angle variable conjugate to $L_{\rm cm}$ (an azimuthal angle). Here we have used the fact that $E_{\rm cm}(I_z,L_{\rm cm},I_r)$ is a Hamiltonian written in terms of the canonical momenta $(I_z,L_{\rm cm},I_r)$. In relating ω_r to the effective cyclotron frequency, one must remember that the radial oscillations are superimposed on the azimuthal motion. The effective cyclotron frequency in the laboratory frame is $\omega_c=\omega_r+\omega_m=\Omega_c/2+\sqrt{(\Omega_c/2)^2-\omega_z^2/2}$. Formally, the parallel action is defined through the equation $\omega_z I_z=M\dot{Z}^2/2+M\omega_z^2Z^2/2$, and the angular momentum $L_{\rm cm}$ is defined in Eq. (203), so Eq. (204) itself defines the action I_r. An alternate discussion of these constants of the motion (using Newton's second law, rather than the Hamilton–Jacobi equation) can be found in the review article by Brown and Gabrielse.[17]

Under ideal conditions, $E_{\rm total}$, $L_{\rm total}$, I_z, $L_{\rm cm}$, and I_c are all conserved exactly, but for a real plasma in a real trap these quantities evolve slowly in time. When the time scale for this evolution is slow compared to the time for Coulomb collisions to bring the plasma particles into thermal equilibrium with each other, a thermodynamic description makes sense. One should picture here a spheroidal plasma that is in thermal equilibrium in terms of its coordinates and velocities relative to the center of mass, but for which the center of mass is undergoing parallel, magnetron, and cyclotron motion.

The center-of-mass motion involves only three degrees of freedom and, consequently, makes negligible contributions to the entropy, that is, $S_{\rm total}=S$. Here $S=S(E,L)$ is the entropy of a plasma at rest with energy E and angular momentum L, that is, $S(E,L)$ is the same entropy function that we considered previously. Combining the equation $TdS_{\rm total}=TdS$ with Eqs. (47), (200), (201), and (204) yields the total differential

$$TdS_{\rm total}=dE_{\rm total}+\omega dL_{\rm total}-\omega_z dI_z+(\omega_m-\omega)dL_{\rm cm} -\omega_r dI_r, \tag{205}$$

where we have assumed that the trap parameters and particle number are held fixed (i.e., $d\omega_z=dB=dN=0$). The rotation frequency $\omega = T\partial S/\partial L)_E = T\partial S_{\rm total}/\partial L_{\rm total})_{E_{\rm total},I_z,L_{\rm cm},I_r}$ has the same interpretation as in previous sections: it is the frequency at which the plasma rotates about the center of mass, as seen from an inertial frame of reference. The total differentials for other thermodynamic potentials (e.g., $F_{\rm total} = E_{\rm total} - S_{\rm total}T$) are obtained by making Legendre transformations.

As a simple application of Eq. (205), suppose that weak anharmonicity in the trap potential leads to slow changes in I_z, I_m, and I_r through weak coupling of the center-of-mass motion to the many other degrees of freedom. The anharmonicity does not break the cylindrical symmetry of the trap, so both $L_{\rm total}$ and $E_{\rm total}$ are constant on the time scale of interest. Thus Eq. (205) plus the second law implies that

$$0 \leqslant TdS_{\rm total} = -\omega_z dI_z - (\omega - \omega_m)dL_{\rm cm} - \omega_r dI_r. \qquad (206)$$

This is a constraint on the direction of evolution in the space of the actions $(I_z, L_{\rm cm}, I_r)$. The evolution is such as to reduce the center-of-mass energy as viewed in the rotating frame of the plasma [i.e., $dE_{\rm cm}/dt + \omega dL_{\rm cm}/dt \leqslant 0$]. The other degrees of freedom impose a kind of ''friction'' on the center-of-mass motion.

B. $m=1$ diocotron motion of a long, thin plasma in a cylindrical trap

As another example, we consider a long, thin plasma that undergoes $m=1$ diocotron motion in a trap of the form shown in Fig. 1. The plasma radius and length are assumed to be ordered as $R_p \ll R_w \ll l_p$, where R_w is the radius of the cylindrical wall. The cyclotron frequency is assumed to be sufficiently large (i.e., $\omega_p \ll \Omega_c$) that the center-of-mass motion transverse to the magnetic field separates cleanly into drift and cyclotron motion. We suppose that external perturbations of the plasma are slow compared to Ω_c, so only the drift motion is excited. In particular, when the plasma is displaced off the axis of the cylindrical trap, the plasma experiences an electric field due to its image in the wall and undergoes $\mathbf{E}\times\mathbf{B}$ drift motion around the center of the trap. This motion of the plasma center of mass is called diocotron motion; it is similar to the magnetron motion discussed above, except that here the electric field causing the drift is an image field, rather than the trap field.

We assume that displacement of the center of mass off axis is small compared to the distance to the wall (i.e., $R \ll R_w$). This together with the ordering $R_p \ll R_w$ implies that the image field is nearly uniform over the cross section of the plasma. The drift motion then translates the plasma as a whole with very little distortion, so the plasma can come to a state of thermal equilibrium (or near equilibrium) centered on the moving center of mass.

The extra energy associated with the displacement is the electrostatic energy of interaction with the image[40]

$$E_{\rm cm} = \frac{(Ne)^2}{l_p} \ln\left(1 - \frac{R^2}{R_w^2}\right). \qquad (207)$$

The kinetic energy associated with the center-of-mass motion is negligible in the drift approximation. Likewise, the canonical angular momentum is dominated by the vector potential contribution

$$L_{\rm cm} = \frac{NeB}{2c} R^2. \qquad (208)$$

By combining these two equations we obtain $E_{\rm cm}(L_{\rm cm})$, which can be thought of as the Hamiltonian for the center-of-mass motion.[40] Thus the center of mass moves around the center of the trap with the angular frequency

$$\omega_D(R) = -\dot{\Theta} = -\frac{\partial E_{\rm cm}}{\partial L_{\rm cm}} = \frac{2Nec}{l_p B R_w^2} \frac{1}{(1 - R^2/R_w^2)}. \qquad (209)$$

In the limit where $R/R_w \rightarrow 0$, this is the well-known frequency of the $m=1$ diocotron mode, and the finite R^2/R_w^2 correction is simply the nonlinear frequency shift.

To develop a thermodynamic description, we again use the equations

$$E_{\rm total} = E_{\rm cm} + E, \qquad (210)$$

$$L_{\rm total} = L_{\rm cm} + L, \qquad (211)$$

$$S_{\rm total} = S(E,L). \qquad (212)$$

Equation (47) then implies the total differential

$$TdS_{\rm total} = dE_{\rm total} + \omega dL_{\rm total} + (\omega_D - \omega)dL_{\rm cm}. \qquad (213)$$

There is an effect called rotational pumping[41,42] that weakly couples the center-of-mass motion to the other degrees of freedom while conserving the total energy and angular momentum. Setting $dE_{\rm total} = dL_{\rm total} = 0$ in Eq. (213) and using the second law yields the result

$$0 \leqslant TdS_{\rm total} = (\omega_D - \omega)dL_{\rm cm}. \qquad (214)$$

When $R/R_w \ll 1$ Eq. (209) implies that ω_D equals the $\mathbf{E}\times\mathbf{B}$ rotation frequency due to the plasma space charge, measured at the wall. Since ω is greater than or equal to the $\mathbf{E}\times\mathbf{B}$ rotation frequency measured in the plasma (due to the addition of the diamagnetic drift) and the electric field in the plasma is greater than the field at the wall, $(\omega_D - \omega)$ must be negative when $R/R_w \ll 1$. It then follows from Eq. (214) that $dL_{\rm cm} = (eB/c)RdR$ is negative, that is, that the plasma moves back toward the center of the trap. Setting $dL_{\rm total} = 0$ in Eq. (211) then implies that $0 \leqslant dL \simeq m(\Omega_c/2)Nd\langle r^2\rangle$, that is, that the plasma expands in radius.

To make further progress, we must specify the mechanism of rotational pumping in more detail. Consider a plasma that has been displaced off axis. Relative to an axis through the plasma center of mass, the end confinement potentials are azimuthally asymmetric. (Of course, these potentials are still symmetric relative to the trap axis.) As a plasma filled flux tube rotates about the plasma axis, the tube is alternately compressed and expanded in length. This rotational pumping alternately increases and decreases $T_\parallel$, the temperature for velocity components parallel to Bz. However, collisions constantly try to maintain equipartition between $T_\parallel$ and $T_\perp$, so there is dissipation of electrostatic energy into heat. A simple estimate for the case where the Debye length is small yields the heating rate

$$\frac{3}{2} Nk\dot{T}=\nu_{\parallel,\perp} NkT\kappa^2\left(\frac{R_pR}{l_pR_w}\right)^2, \tag{215}$$

where $\nu_{\parallel,\perp}$ is the collisional equipartition rate and κ is a numerical constant of order unity.[41,42]

Given this heating rate, thermodynamics can be used to determine the rate of plasma evolution [e.g., $\dot{R}$ and $\dot{\omega}$]. Since rotational pumping conserves the total energy and angular momentum, Eqs. (208)–(211) imply that

$$0=\dot{E}_{\text{total}}=\dot{E}-\omega_D m\Omega_c NR\dot{R}, \tag{216}$$

$$0=\dot{L}_{\text{total}}=\dot{L}+m\Omega_c NR\dot{R}. \tag{217}$$

Also, $\dot{E}$ and $\dot{L}$ are still related to $\dot{T}$ and $\dot{\omega}$ through evolution equations (174) and (175), which for the case of weak correlation and low rotation frequency (i.e., $\omega \ll \omega_c$) reduce to the simple form

$$\frac{3}{2} Nk\dot{T}=\omega\dot{L}+\dot{E}, \tag{218}$$

$$\dot{\omega}\,\frac{\partial L}{\partial\omega}\,\omega=\omega\dot{L}-Nk\dot{T}. \tag{219}$$

Combining Eqs. (216)–(218) yields the relation

$$\frac{3}{2} Nk\dot{T}=(\omega_D-\omega)m\Omega_c NR\dot{R}, \tag{220}$$

and then using heating rate (215) to evaluate $\dot{T}$ provides the rate at which the plasma center of mass moves back toward the axis of the trap

$$\frac{\dot{R}}{R}\equiv-\gamma=-\frac{\nu_{\parallel,\perp}kT\kappa^2R_p^2}{m\Omega_c(\omega-\omega_D)l_p^2R_w^2}. \tag{221}$$

Since $R(t)$ can be thought of as the amplitude of an $m=1$ diocotron mode that is excited on the plasma, γ is the mode damping decrement due to rotational pumping.[41,42] Substituting $\dot{L}\simeq m(\Omega_c/2)Nd\langle r^2\rangle/dt$ into Eq. (217) yields an expression for the plasma expansion rate

$$\frac{d\langle r^2\rangle}{dt}=2\gamma R^2, \tag{222}$$

and combining Eqs. (141) and (217)–(221) yields the evolution rate of the plasma rotation frequency

$$\frac{\dot{\omega}}{\omega}=-\left(\frac{4}{3}+\frac{8}{3}\frac{\omega_D}{\omega}\right)\frac{R^2}{R_p^2}\,\gamma. \tag{223}$$

A comparison between Eqs. (222) and (223) illustrates a subtle point concerning the approximations used here. From the relations $\omega_p^2\simeq 2\omega\Omega_c$ and $N=\pi nR_p^2l_p$ we obtain

$$\frac{\dot{R}_p}{R_p}=-\frac{1}{2}\frac{\dot{n}}{n}=-\frac{1}{2}\frac{\dot{\omega}}{\omega}, \tag{224}$$

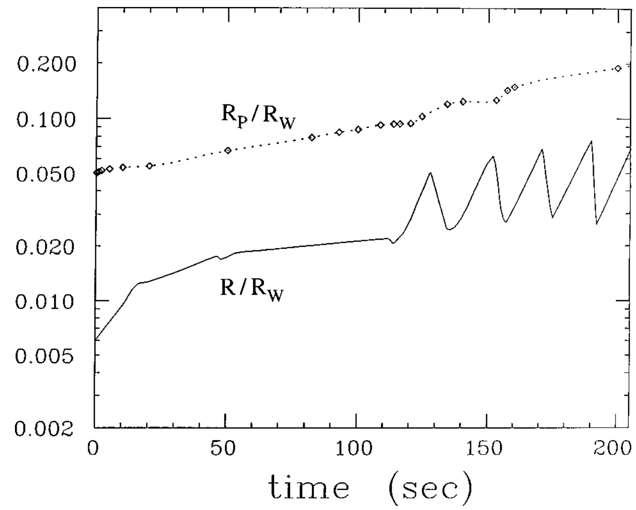

FIG. 10. Measured evolution of the plasma radius R_p and displacement off-axis R (both scaled by the wall radius R_w). Taken from Cluggish *et al.* (Ref. 13).

which would contradict Eq. (222) if we set $d\langle r^2\rangle/dt=R_p\dot{R}_p$. However, by referring to Eq. (148) and noting that $\langle r^2\rangle^{(0)}=R_p^2/2$, one can see that

$$\frac{d}{dt}\langle r^2\rangle=R_p\dot{R}_p+\frac{d}{dt}\frac{kT}{\pi ne^2}. \tag{225}$$

By using $\dot{n}/n=\dot{\omega}/\omega$ and Eqs. (220) and (223) to evaluate the second turn on the right-hand side, Eqs. (225) and (224) are seen to be consistent.

The mode damping rate (221) and expansion rate (222) were derived earlier from a transport perspective,[41] before any connection to thermodynamics was realized. Also, the rates were found to be in good agreement with experiment.[42] In particular the temperature dependence of $\gamma(T)$, which is the same as that of heating rate (215), was checked over several decades variation in T.

Interestingly, $\gamma(T)$ is an increasing function of T for low T, which is the kind of temperature dependence in a heating rate that can give rise to a temperature instability [see Eq. (189)]. Qualitatively, the temperature dependence is easy to understand. For large T, $\nu_{\parallel,\perp}T\propto T^{-1/2}$ is a decreasing function. However, for a temperature sufficiently low that $\sqrt{kT/m}/\Omega_c=r_c\ll b=e^2/kT$, the cyclotron adiabatic invariant constrains the collisional dynamics and $\nu_{\parallel,\perp}$ becomes exponentially small.[43] Thus $\gamma(T)$ is an increasing function for low T reaching a peak near the temperature where $r_c=b$.

The temperature instability has been used to explain a limit cycle behavior that is observed with $m=1$ diocotron modes.[13] Figure 10 shows the observed amplitude of the mode and plasma radius versus time for an elapsed time of 300 s, which is about a million periods of the basic diocotron motion. The sawtooth oscillations of the mode amplitude is a manifestation of the limit cycle.

In the experiments, the diocotron mode is made unstable to the resistive wall instability by inserting resistors between azimuthally separated sections of the conducting wall. There is a competition between resistive growth of the mode and damping due to rotational pumping. Likewise, the temperature evolution involves a competition between rotational pumping, which transforms electrostatic energy into heat and cooling due to cyclotron radiation.

The resistors change the total angular momentum at the rate

$$\dot{L}_{\mathrm{total}}=2\beta L_{\mathrm{cm}}=2\beta\,\frac{m\Omega_c}{2}\,NR^2, \tag{226}$$

where β is a constant determined by the wall impedance.[13] Likewise, the resistors change the total energy at the rate $(\partial E_{\mathrm{cm}}/\partial L_{\mathrm{cm}})2\beta L_{\mathrm{cm}}=-\omega_D 2\beta L_{\mathrm{cm}}$. Also taking into account the energy loss by cyclotron radiation yields the rate

$$\dot{E}_{\mathrm{total}}=-2\beta\omega_D\,\frac{m\Omega_c}{2}\,NR^2-\frac{3}{2}\,Nk\,\frac{(T-T_w)}{\tau_{\mathrm{rad}}}, \tag{227}$$

where τ_{rad} is the radiative rate and T_w is the temperature of the wall. The cyclotron radiation makes negligible change in the angular momentum; for a single photon, $\delta L=\hbar$ and $\delta E=\hbar\Omega_c$ so $\omega\,\delta L/\delta E=\omega/\Omega_c\ll 1$. For the conditions of the experiment, $\beta\simeq 0.1\ \mathrm{s}^{-1}$ and $\tau_{\mathrm{rad}}\simeq 0.29$ s.

Also, we know the rate at which rotational pumping and cyclotron radiation change the plasma temperature. From heating rate (215) and the definition of γ in Eq. (221), we obtain

$$\frac{3}{2}\,Nk\dot{T}=2\gamma(\omega-\omega_D)\,\frac{m\Omega_c}{2}\,NR^2-\frac{3}{2}\,Nk\,\frac{(T-T_w)}{\tau_{\mathrm{rad}}}. \tag{228}$$

Equations (208)–(211) and (218) imply that

$$\dot{E}_{\mathrm{total}}+\omega\dot{L}_{\mathrm{total}}=\frac{3}{2}\,Nk\dot{T}+(\omega-\omega_D)m\Omega_c NR\dot{R}. \tag{229}$$

Using Eqs. (226), (227), and (228) to replace $\dot{E}_{\mathrm{total}}$, $\dot{L}_{\mathrm{total}}$, and $\dot{T}$ then yields the result

$$\dot{R}=(\beta-\gamma)R, \tag{230}$$

where $\gamma=\gamma(T,R_p)$ is given in Eq. (221). Using this result together with Eqs. (221) and (226) yields the expansion rate

$$\frac{d}{dt}\,\langle r^2\rangle=2\gamma R^2, \tag{231}$$

or its integral equivalent

$$\langle r^2\rangle(t)=\langle r^2\rangle(0)+\int_0^{\pm}2\gamma R^2 dt. \tag{232}$$

If the cyclotron radiation maintains the temperature at a sufficiently low level (i.e., $\lambda_D\ll R_p$), then we can approximate $\langle r^2\rangle(t)$ by $\langle r^2\rangle^{(0)}(t)=R_p^2(t)/2$ in this last relation. Furthermore, the evolution of R_p is related to the evolution of the rotation frequency through Eq. (224).

Equations (228), (230), and (232) are three coupled equations that determine the evolution of T, R, and R_p. These equations were obtained earlier, but not put in a thermodynamics context. Numerical integration and analytical analysis of the equations show that they explain the limit cycle behavior exhibited in Fig. 10.[13]

To understand the importance of the temperature instability in this behavior, we first note that for sufficiently small R, Eq. (232) describes a very gradual monotonic increase in $R_p(t)$. This gradual increase can be seen in Fig. 10. Over a single cycle, we can treat $R_p(t)$ as constant and consider only the coupling between T and R through Eqs. (228) and (230).

Following the previous analysis, we write these equations as

$$\frac{d}{dt}\,\mathbf{T}=\gamma(\mathbf{T})\mathbf{R}^2-\frac{\mathbf{T}}{\tau_{\mathrm{rad}}}, \tag{233}$$

$$\frac{d}{dt}\,\mathbf{R}^2=2[\beta-\gamma(\mathbf{T})]\mathbf{R}^2, \tag{234}$$

where

$$\mathbf{T}=\frac{3k}{2}\,(T-T_w) \tag{235}$$

and

$$\mathbf{R}^2=2(\omega-\omega_D)\,\frac{m\Omega_c}{2}\,R^2. \tag{236}$$

Note that ω is constant for constant R_p and ω_D is constant for sufficiently small R.

For the conditions of the experiment (i.e., $\beta\tau_{\mathrm{rad}}\ll 1$), the intrinsic evolution of $\mathbf{T}$ is much faster than the evolution of $\mathbf{R}$, so for most of the time $\mathbf{T}$ has relaxed to an equilibrium $\mathbf{T}^*(\mathbf{R})$ determined by

$$0=\gamma(\mathbf{T}^*)\mathbf{R}^2-\frac{\mathbf{T}^*}{\tau_{\mathrm{rad}}}. \tag{237}$$

This temperature equilibrium is stable provided that

$$\frac{d\gamma}{d\mathbf{T}^*}\,\mathbf{R}^2-\frac{1}{\tau_{\mathrm{rad}}}\leqslant 0. \tag{238}$$

However, as $\mathbf{R}$ continues to evolve, a stability boundary is reached where $d\gamma/d\mathbf{T}^*-1/\tau_{\mathrm{rad}}$ passes through zero. $\mathbf{T}$ then evolves rapidly (jumps) to the next stable region. During this rapid evolution, the change in $\mathbf{R}$ is negligible.

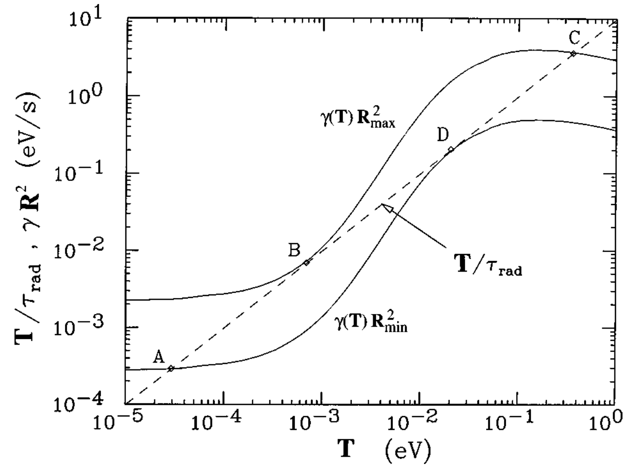

FIG. 11. Changes in **R** and **T** during a limit cycle. The cooling rate (dashed curve) depends only on **T**. The heating rate depends on both **T** and **R**; the solid curves show the heating rate at the maximum and minimum values of **R** during the limit cycle. Taken from Cluggish *et al.* (Ref. 13).

A limit cycle [sawtooth oscillation in Fig. 10] is illustrated in Fig. 11. The two solid curves are plots of $\gamma(\mathbf{T})\mathbf{R}^2$ versus $\mathbf{T}$ for $\mathbf{R}=\mathbf{R}_{\max}$ (top of sawtooth) and $\mathbf{R}=\mathbf{R}_{\min}$ (bottom of sawtooth), and the dashed curve is simply $\mathbf{T}/\tau_{\mathrm{rad}}$. The cycle starts at point A, where both $\mathbf{T}$ and $\mathbf{R}$ take their minimum values. At this point, inequality (238) is satisfied so $\mathbf{T}$ is in a stable equilibrium. However, β is larger than $\gamma(\mathbf{T})$ so $\mathbf{R}$ grows. The equilibrium temperature $\mathbf{T}=\mathbf{T}^*(\mathbf{R})$ tracks the growth of $\mathbf{R}$ according to Eq. (237). During this phase, the system evolves to point B where $R=R_{\max}$. At this point, the temperature becomes unstable and evolves rapidly up to point C, the next stable equilibrium. The value of $\mathbf{R}$ does not change significantly during this phase of the evolution, that is, $\mathbf{R}=\mathbf{R}_{\max}$ for both point B and point C. Now $\gamma(\mathbf{T})$ is larger than β, so $\mathbf{R}$ begins to decrease, and again the stable temperature equilibrium $\mathbf{T}=\mathbf{T}^*(\mathbf{R})$ tracks the decrease according to Eq. (237). During this phase the system evolves to point D, where $\mathbf{R}=\mathbf{R}_{\min}$. Here the temperature becomes unstable and evolves rapidly to the next stable equilibrium at point A, and that completes the cycle.

VIII. CONCLUSIONS

Plasmas that consist exclusively of particles with a single sign of charge can be confined by static electric and magnetic fields (in a Penning trap) and also be in a state of global thermal equilibrium. The possibility of using the powerful techniques of thermal equilibrium statistical mechanics to describe the plasma state is a huge advantage. Gibbs solves the complicated many body physics problem for us. We began this paper with a brief review of the conditions for and structure of the thermal equilibrium states. The interested reader can find a more detailed description of these states, including a discussion of microscopic order and of phase transitions, in the new review article: ''Nonneutral plasmas, liquids, and crystals (The thermal equilibrium states).''[5]

Next we developed a thermodynamic theory of the trapped plasmas. The main advantage of such a theory is that it provides a large reduction in the level of complexity required to specify the plasma state. Without loss of generality the state is specified by any complete set of thermodynamic variables (a few numbers). The theory provides many general relations (Maxwell relations) between partial derivatives of the thermodynamic variables with respect to one another. Thermodynamic inequalities place useful and general bounds on certain partial derivatives. General and relatively simple expressions are provided for fluctuations in the values of the thermodynamic variables. Often plasmas are made to evolve through a sequence of thermal equilibrium states by the slow addition (or subtraction) of energy and angular momentum, for example, through the interaction with neutrals or deliberately applied laser beams. A thermodynamic approach provides a simple description of such evolution through two coupled ordinary differential equations for the time dependence of the plasma temperature and rotation frequency. These equations provide a theoretical basis for the late time dynamical control of trapped plasmas. Finally, for certain special situations, there are extra constants of motion associated with the plasma center-of-mass motion, and these enter the theory as additional thermodynamic variables. As a simple application, this extended theory was used to describe a limit cycle behavior observed with pure electron plasmas.

In general, this whole subject is very large, and there is much room (and need) for future work. For example, only a few of the hundreds of Maxwell relations have been explored. Only a reduced set of thermodynamic inequalities was obtained, and only two of these [i.e., $c_L \geqslant 0$ and $(\partial\omega/\partial L)_T \leqslant 0$] were used in any serious way. The method for calculating fluctuations was illustrated with a couple of examples, but was not exploited, say, to discover new diagnostics based on the measurement of fluctuations. Our work should be thought of as simply a framework for future work. Our hope is that the framework and the few applications worked out will provide adequate guidance for other authors, particularly experimentalists, to develop the applications they need.

We single out experimentalists here for special encouragement because in other areas of research where thermodynamics plays a prominent role (e.g., low-temperature condensed matter physics) the experimentalists are often the expert practitioners. For example, they use thermodynamics to guide (or condition) their choice of measurement and to relate the measurement of one quantity to other quantities of interest (through Maxwell relations). A simple example from transport illustrates how thermodynamics can help guide the choice of measurement. Suppose that a trapped plasma is slowly evolving (through a sequence of thermal equilibrium states) as a result of the interaction with a small static field error. Over the years, the non-neutral plasma community has investigated the influence of such a field asymmetry by measuring various quantities: the time required for the plasma radius to double, the time for the central density to drop by a factor of 2, etc. However, a thermodynamic approach makes it clear that the plasma evolution is controlled by the rate of change of the plasma energy and angular momentum (i.e., $\dot{E}$ and $\dot{L}$). A static field asymmetry cannot change the plasma energy, so the only aspect of the field error that matters is the torque it applies on the plasma. The task of experiment is to measure the torque, and the task of theory is to calculate the torque. Simply by using a thermodynamic framework, we are forced to focus on the important physical quantity.

ACKNOWLEDGMENTS

The authors wish to thank Francois Anderegg, John Bollinger, Steve Crooks, Fred Driscoll, Pei Huang, and Brian Cluggish for useful discussions.

This work was supported by National Science Foundation Grant No. PHY94-21318 and Office of Naval Research Grant No. N00014-96-1-0239.

[1] J. J. Bollinger, D. J. Wineland, and D. H. E. Dubin, Phys. Plasmas **1**, 1403 (1994).
[2] D. J. Heinzen, J. J. Bollinger, F. L. Moore, W. M. Itano, and D. J. Wineland, Phys. Rev. Lett. **66**, 2080 (1991); J. J. Bollinger, D. J. Heinzen, F. L. Moore, W. M. Itano, D. J. Wineland, and D. H. E. Dubin, Phys. Rev. A **48**, 525 (1993).

[3]X.-P. Huang, F. Anderegg, E. M. Hollmann, C. F. Driscoll, and T. M. O'Neil, Phys. Rev. Lett. **78**, 875 (1997).
[4]X.-P. Huang, J. J. Bollinger, T. B. Mitchell, and W. M. Itano, Phys. Rev. Lett. **80**, 73 (1998).
[5]A proof of this often quoted result can be found in a new review article: Daniel H. E. Dubin and T. M. O'Neil, ''Trapped nonneutral plasmas, liquids, and crystals (The thermal equilibrium states),'' submitted to Rev. Mod. Phys. Portions of the review article are reproduced and extended here in order to present a unified exposition of the thermodynamics of nonneutral plasmas, with particular emphasis on the thermodynamics of transport processes.
[6]T. M. O'Neil and C. F. Driscoll, Phys. Fluids **22**, 266 (1979).
[7]N. R. Corngold, Prog. Astronaut. Aeronaut. **158**, 583 (1994).
[8]D. H. E. Dubin and T. M. O'Neil, Phys. Rev. Lett. **56**, 728 (1986).
[9]R. A. Smith, Phys. Rev. Lett. **63**, 1479 (1989).
[10]R. A. Smith and T. M. O'Neil, Phys. Fluids B **2**, 2961 (1990).
[11]S. Ichimaru, Rev. Mod. Phys. **54**, 1017 (1982).
[12]J. P. Hansen, Phys. Rev. A **8**, 3096 (1973); E. L. Pollock and J. P. Hansen, *ibid.* **8**, 3110 (1973).
[13]B. P. Cluggish and C. F. Driscoll, Phys. Plasmas **3**, 1813 (1996); B. P. Cluggish, C. F. Driscoll, K. Avinash, and J. Helffrich, *ibid.* **4**, 2062 (1997).
[14]F. M. Penning, Physica (Amsterdam) **3**, 873 (1936).
[15]J. S. deGrassie and J. H. Malmberg, Phys. Rev. Lett. **39**, 1077 (1977); J. S. deGrassie and J. H. Malmberg, Phys. Fluids **23**, 63 (1980).
[16]H. G. Dehmelt, Adv. At. Mol. Phys. **32**, 53 (1967).
[17]L. S. Brown and G. Gabrielse, Rev. Mod. Phys. **58**, 233 (1986).
[18]L. D. Landau and E. M. Lifshitz, *Mechanics* (Addison-Wesley, Reading, MA, 1960), p. 129.
[19]L. D. Landau and E. M. Lifshitz, *Statistical Physics* (Pergamon, London, 1958).
[20]F. Reif, *Fundamentals of Statistical and Thermal Physics* (McGraw-Hill, New York, 1965), p. 221.
[21]R. C. Davidson and N. A. Krall, Phys. Fluids **13**, 1543 (1970).
[22]R. C. Davidson, *Physics of Nonneutral Plasmas* (Addison-Wesley, Redwood City, CA, 1990), p. 110.
[23]S. A. Prasad and T. M. O'Neil, Phys. Fluids **22**, 278 (1979); T. M. O'Neil and C. F. Driscoll, *ibid.* **22**, 266 (1979).
[24]J. H. Malmberg and T. M. O'Neil, Phys. Rev. Lett. **39**, 1333 (1977).
[25]J. R. Brewer, J. D. Prestage, J. J. Bollinger, W. M. Itano, D. J. Larson, and D. J. Wineland, Phys. Rev. A **38**, 859 (1988).
[26]D. H. E. Dubin and T. M. O'Neil, Phys. Rev. Lett. **60**, 511 (1988); A. Rahman and J. P. Schiffer, *ibid.* **57**, 1133 (1986); J. P. Schiffer, in *Nonneutral Plasma Physics II*, edited by J. Fajans and D. H. E. Dubin AIP Conf. Proc. No. 331 (American Institute of Physics, New York, 1995), p. 191.
[27]C. F. Driscoll, J. H. Malmberg, and K. S. Fine, Phys. Rev. Lett. **60**, 1290 (1988).
[28]D. H. E. Dubin and T. M. O'Neil, Phys. Fluids **29**, 11 (1986).
[29]X.-P. Huang, J. Tan, J. J. Bollinger, and D. J. Wineland (personal communication, 1997).
[30]R. K. Pathria, *Statistical Mechanics* (Pergamon, Oxford, 1986), p. 97.
[31]J. L. Leibowitz, J. K. Pereus, and L. Verlet, Phys. Rev. **153**, 250 (1967).
[32]D. H. E. Dubin, Phys. Rev. A **40**, 1140 (1989).
[33]M. W. Zemansky, *Heat and Thermodynamics*, 5th ed. (McGraw-Hill, New York, 1968), p. 287.
[34]D. H. E. Dubin, Phys. Rev. E **53**, 5268 (1996).
[35]R. C. Davidson and S. M. Lund, *Advances in Plasma Physics, Thomas H. Stix Symposium*, edited by N. J. Fisch (American Institute of Physics, New York, 1993), p. 1.
[36]N. R. Corngold, Phys. Fluids B **5**, 3847 (1993).
[37]D. J. Wineland and W. M. Itano, Phys. Rev. A **20**, 1521 (1979).
[38]D. J. Wineland, J. J. Bollinger, W. M. Itano, and J. D. Prestage, J. Opt. Soc. Am. B **2**, 1721 (1985).
[39]D. J. Wineland and H. G. Dehmelt, J. Appl. Phys. **46**, 919 (1975).
[40]T. M. O'Neil and R. A. Smith, Phys. Fluids B **4**, 2720 (1992).
[41]S. M. Crooks and T. M. O'Neil, Phys. Plasmas **2**, 355 (1995).
[42]B. P. Cluggish and C. F. Driscoll, Phys. Rev. Lett. **74**, 4213 (1995).
[43]T. M. O'Neil and P. G. Hjorth, Phys. Fluids **28**, 3241 (1985); M. E. Glinsky, T. M. O'Neil, M. N. Rosenbluth, K. Tsuruta, and S. Ichimaru, Phys. Fluids B **4**, 2720 (1992); B. R. Beck, J. Fajans, and J. H. Malmberg, Phys. Rev. Lett. **68**, 317 (1992).